Accurate Langevin approaches to simulate Markovian channel dynamics

2015 Phys. Biol. 12 061001

(http://iopscience.iop.org/1478-3975/12/6/061001)

IOP Publishing Phys. Biol. 12 (2015) 061001 doi:10.1088/1478-3975/12/6/061001

Physical Biology

TOPICAL REVIEW

Accurate Langevin approaches to simulate Markovian channel dynamics

Yandong Huang[1], **Sten Rüdiger**[2] **and Jianwei Shuai**[3]

[1] Department of Physics, Xiamen University, Xiamen 361005, People's Republic of China
[2] Institute of Physics, Humboldt-Universität zu Berlin, Berlin, Germany
[3] Department of Physics and State Key Laboratory of Cellular Stress Biology, Innovation Center for Cell Signaling Network, Xiamen University, Xiamen 361005, People's Republic of China

E-mail: sten.ruediger@physik.hu-berlin.de **and** jianweishuai@xmu.edu.cn

RECEIVED
7 June 2015

ACCEPTED FOR PUBLICATION
18 August 2015

PUBLISHED
25 September 2015

Keywords: neuron model, channel dynamics, Langevin approach, stochastic dynamics

Abstract

The stochasticity of ion-channels dynamic is significant for physiological processes on neuronal cell membranes. Microscopic simulations of the ion-channel gating with Markov chains can be considered to be an accurate standard. However, such Markovian simulations are computationally demanding for membrane areas of physiologically relevant sizes, which makes the noise-approximating or Langevin equation methods advantageous in many cases. In this review, we discuss the Langevin-like approaches, including the channel-based and simplified subunit-based stochastic differential equations proposed by Fox and Lu, and the effective Langevin approaches in which colored noise is added to deterministic differential equations. In the framework of Fox and Lu's classical models, several variants of numerical algorithms, which have been recently developed to improve accuracy as well as efficiency, are also discussed. Through the comparison of different simulation algorithms of ion-channel noise with the standard Markovian simulation, we aim to reveal the extent to which the existing Langevin-like methods approximate results using Markovian methods. Open questions for future studies are also discussed.

1. Introduction

The propagation of action potentials is considered the most important type of neuronal signaling. Generation of action potentials and their transmission through the axon are governed by currents through ion channels on the neuronal membrane [1]. Hodgkin and Huxley first described the nerve membrane ion currents deterministically and established what is now called the Hodgkin–Huxley (HH) model [2]. The classical HH model is expressed by a set of differential equations to provide a deterministic description of the mean gating states of ion channels and predicts a voltage dynamics closely resembling the membrane potential spikes observed in neurons. It was then suggested that the underlying gating behavior is subject to internal noise from microscopic fluctuations [3, 4]. The stochastic channel dynamics was confirmed later directly by single channel current recordings with the patch clamp techniques developed by Neher and Sakmann [5–7].

Early experiments indicated that channel noise may be particularly important in small neuronal structures such as the nodes of Ranvier [8]. Large channel noise has been implicated in limiting the reliability of neuronal responses to repeated presentations of identical stimuli and the reliability of action potential propagation in thin axons [9–12]. However, it has been realized that suitable channel noise might also be exploited by nervous systems in order to improve the neural signaling transmission and procession. Simulation studies have shown that channel noise can induce many nontrivial effects in neural systems. These deviations from deterministic prediction include spontaneous action potential generation [13–17], firing time variability [9, 18, 19], firing rate increasing with the number of ion channels [15, 16, 20], stochastic resonance [21–24], coherence resonance [22, 25, 26], entropically enhanced excitability [27, 28], spike firing patterns [29], stochastic facilitation [30] and others [31–38]. Besides neuronal dynamics, channel noise is also ubiquitous in a host of other cellular processes

including signaling in electrically non-excitable cells, for instance the intracellular calcium release from the endoplasmic reticulum (ER) through stochastic inositol 1,4,5-trisphosphate receptor (IP_3R), [39–48] and from the sarcoplasmic reticulum through stochastic ryanodine receptors [49–51].

The channel noise originates from fluctuations in the gating transitions because of the discrete nature of partaking molecules and it becomes influential when the number of reacting particles is small. In those circumstances, the standard representation of chemical reactions, namely the differential equations based on the law of mass action, can be replaced by the master equation approach, where the reactions or gating transitions are treated as a Markovian birth–death process [22, 27, 39, 41, 46]. Simulations demonstrated that the HH neuron model with Markovian stochastic channels can generate the known macroscopic electrical properties of neurons, including resting potentials, action potentials, subthreshold spike generation, and chaotic behaviors [13, 14]. The Markovian method can thus be considered as the standard method for the simulation of ion-channel dynamics and can be exactly simulated via a Gillespie-type algorithm [52–54]. However, these Markovian methods are computationally demanding in the case of large channel numbers, making approximate methods favorable.

As in other systems one is therefore interested in an efficiently tractable modeling. Therefore, a central question for the stochastic HH approach and similar conductance-based models is that for the efficient incorporation of channel noise. The Langevin approach is often used to approximate the master equation for finite channel numbers. For the HH equations, this idea was introduced by Fox and Lu, who used a Kramers–Moyal expansion to derive stochastic differential equation (SDE) models [15, 20]. This approach has been often used in the last two decades and thus the issue of channel noise in the HH equations appeared to be settled. Yet, over the last five years or so, a number of studies have appeared to discuss modified HH Langevin equations.

Why is there a need for such further analysis? First, it was found early that in certain cases the classical Fox and Lu approach based on subunits lacks accuracy when compared to the numerical solution of master equations. This holds particularly for the case of small-to-moderate channel numbers, which has attracted interest related to the research on optimal nerve cell design [11]. However, even for large channel numbers, there are systematic deviations from the discrete simulations [55–58]. In the course of these studies the reason for the deviations was sought and located in the coupling of gating variables. Briefly, in the HH model, the gating of an ion channel is governed by the states of its subunits. All subunits in a channel are assumed statistically independent. Each subunit has two discrete configuration states, i.e. the activation (open) and non-activation (closed) states, and randomly transitions between the two configurations. In the framework of Fox and Lu, two classes of approximations, termed subunit-based approaches and channel-based approaches, were proposed to represent the Markovian channel noise. They are different essentially in the place where channel noise is added to the SDEs. Subunit-based Fox–Lu approaches add Gaussian noise to the equations that describe the fractions of subunit states of channels, while channel-based Fox–Lu approaches introduce Gaussian noise directly into the fractions of channel states. Subunit-based approaches are simpler and require fewer computational resources, which is why they have been applied extensively to stochastic neuron models [33, 59]. However, in comparison with the standard Markov method, subunit-based approaches could not correctly capture the firing dynamics [55–58].

The channel-based Fox–Lu approach was demonstrated to better replicate the statistical properties of the Markovian HH neuron [58]. In the channel-based approach, the dimension of state space is much larger than that in the subunit-based approach and two diffusion matrices have to be defined to calculate noise in the state fractions for the Na^+ and K^+ channels. The diffusion matrix has to be positive semidefinite in order to obtain real valued matrix square roots, which is usually a time-consuming numerical procedure. Nevertheless, the efficient determination of the noise amplitudes in the channel-based approach was reconsidered recently in [60, 61], where a procedure that obviates the square root calculation was used.

A further issue of recent work deals with an inconsistent treatment of channel state fractions in the original channel-based Fox–Lu approach. This problem becomes particularly important when the number of channels is small. Due to the addition of Gaussian noise to the SDEs, the fractions of channel states may be out of the range of [0, 1], which lacks biological meaning. The original channel-based Fox–Lu approach does not consider confinement within the interval [0, 1] for the fractions of the eight states for Na^+ channels and five states for K^+ channels. Until recently, these fractions were allowed to evolve freely without boundary limitation based on the equilibrium noise approximation proposed in the first implementation of this approach by Goldwyn *et al* [58]. Later, two numerical algorithms were devised to make sure the state fractions stay in the unit interval [61, 62].

This review is organized as follows. We first briefly discuss the original HH model in terms of deterministic differential equations and introduce the subunit-based and channel-based approaches. Then, in section 3 we discuss the stochastic modeling using the master equation approach with discrete state variables. Here we also briefly review the numerical algorithms for discrete simulations. Section 4 introduces the standard methods to derive Langevin equations and their application to the subunit- and channel-based approaches. We also discuss in detail the various

recent efforts of efficient Langevin modeling for the two approaches. The open questions for future study are addressed in section 5.

2. Hodgkin–Huxley (HH) Model

In this section, we briefly recapitulate the deterministic HH model [2] and the two basic approaches for channel and subunit modeling. The two approaches lead to equivalent descriptions as long as the deterministic case is considered.

2.1. Deterministic HH Model

A single-compartment HH model is considered, in which the neuronal membrane voltage evolution is governed by [2]

$$-C\frac{\mathrm{d}V}{\mathrm{d}t} = I_{\mathrm{Na}} + I_{\mathrm{K}} + I_{\mathrm{L}} + I_{\mathrm{Stim}}, \tag{1}$$

where V is the membrane voltage in millivolts, C represents the membrane capacitance (usually set to 1 μF cm^{-2}) and I_{Stim} is the stimulus current added to the neuron in μA cm^{-2}. The values of I_{Na}, I_{K}, and I_{L} are the currents of Na^+, K^+, and leakage channels, respectively, given by

$$I_{\mathrm{Na}} = g_{\mathrm{Na}}\rho_{\mathrm{Na}}\left(V - E_{\mathrm{Na}}\right), \tag{2}$$

$$I_{\mathrm{K}} = g_{\mathrm{K}}\rho_{\mathrm{K}}\left(V - E_{\mathrm{K}}\right), \tag{3}$$

and

$$I_{\mathrm{L}} = g_{\mathrm{L}}\left(V - E_{\mathrm{L}}\right), \tag{4}$$

where $E_{\mathrm{Na}} = 50$ mV, $E_{\mathrm{K}} = -77$ mV, and $E_{\mathrm{L}} = -53.4$ mV are the reversal potentials of K^+, Na^+, and leakage channels, respectively, and $g_{\mathrm{Na}} = 120$ ms cm^{-2}, $g_{\mathrm{K}} = 36$ ms cm^{-2}, $g_{\mathrm{L}} = 0.3$ ms cm^{-2} are the total conductances for Na^+, K^+, and leakage currents, respectively. The values ρ_{Na} and ρ_{K} denote the open fractions of Na^+ and K^+ channels respectively. In the HH model, each Na^+ channel contains two types of subunits, including three m subunits and one h subunit. Each K^+ channel is composed by four n subunits. If all four subunits are in the activation (open) state, one defines the Na^+ or K^+ channel to be open.

2.1.1. Subunit-based expression

The original HH model employs the subunit-based expression of open fractions, ρ_{Na} and ρ_{K}, of Na^+ and K^+ channels respectively. Taking the variables m, n, and h as the open fraction of the m, h, and n types of channel subunits, ρ_{Na} and ρ_{K} can be obtained exactly with m^3h and n^4, respectively. The evolution of open fraction $w = \{m, h, n\}$ can be expressed with the relaxation equations:

$$\frac{\mathrm{d}w}{\mathrm{d}t} = \alpha_w(1 - w) - \beta_w w, \text{ where } w = m, h, \text{ or } n. \tag{5}$$

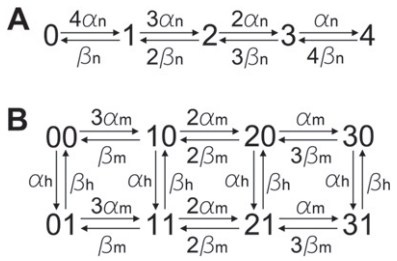

Figure 1. Transition diagrams of (a) K^+ channel states and (b) Na^+ channel states. The code indicates how many subunits in the channel are in the open state. In (a) the code 4 means four opening n subunits and therefore represents the open state of a K^+ channel. In (b) the code 31 means three opening m subunits and one opening h subunit, indicating the open state of a Na^+ channel. The kinetic parameters α and β denote the transition rates between connected channel states.

Here, α_w and β_w are voltage-dependent subunit opening and closing rates with the unit of ms^{-1}. We have

$$\alpha_m = \frac{0.1(V + 40)}{1 - \exp[-(V + 40)/10]}, \tag{6}$$

$$\beta_m = 4\exp[-(V + 65)/18], \tag{7}$$

$$\alpha_h = 0.07\exp[-(V + 65)/20], \tag{8}$$

$$\beta_h = \frac{1}{1 + \exp[-(V + 35)/10]}, \tag{9}$$

for the m_{Na} and h_{Na} subunits of Na^+ channels, and

$$\alpha_n = \frac{0.01(V + 55)}{1 - \exp[-(V + 55)/10]}, \tag{10}$$

$$\beta_n = 0.125\exp[-(V + 65)/80], \tag{11}$$

for n_{K} subunit of K^+ channels.

2.1.2. Channel-based expression

Next, we describe ion-channel open fractions ρ_{Na} and ρ_{K} with the channel-based expression, which is equivalent to the subunit-based expression in the limit of infinitely many channels. Here, the states of an ion channel are regulated by the configurations of multiple subunits and the dynamics through state transitions. For the K^+ channels with four n subunits, a count of open subunits defines a channel state, thus a K^+ channel gets five distinct states, as shown in figure 1(a). As to Na^+ channels, there are two different types of subunits, namely three m subunits and one h subunit, thus the combination of the counts of open m subunits and h subunit defines eight channel states, as shown in figure 1(b).

By considering the mass action kinetics with the transition diagram of channel states, the differential equations that describe the trajectories of channel state fractions are as follows [15, 20]:

$$\rho_{\mathrm{Na}} = y_{3,1}, \tag{12}$$

$$\rho_{\mathrm{K}} = x_4, \tag{13}$$

$$\frac{d\mathbf{Y}}{dt} = A_{Na}\mathbf{Y}, \tag{14}$$

$$\frac{d\mathbf{X}}{dt} = A_{K}\mathbf{X}, \tag{15}$$

where A_{Na} and A_K are transition matrices of Na^+ and K^+ channels respectively, which are derived from the master equation representation of the transition diagrams as illustrated in figure 1. Vectors $Y = \{y_{jk}\}$ with $j = 0, 1, 2, 3$ and $k = 0, 1$ in figure 1(b) and $X = \{x_i\}$ with $i = 0, 1, 2, 3, 4$ in figure 1(a) denote the eight Na^+ channel states and five K^+ channel states, respectively.

The transition matrices A_{Na} and A_K are given as follows

$$A_{Na} = \begin{pmatrix} a_{Na(1)} & \beta_m & 0 & 0 & \beta_h & 0 & 0 & 0 \\ 3\alpha_m & a_{Na(2)} & 2\beta_m & 0 & 0 & \beta_h & 0 & 0 \\ 0 & 2\alpha_m & a_{Na(3)} & 3\beta_m & 0 & 0 & \beta_h & 0 \\ 0 & 0 & \alpha_m & a_{Na(4)} & 0 & 0 & 0 & \beta_h \\ \alpha_h & 0 & 0 & 0 & a_{Na(5)} & \beta_m & 0 & 0 \\ 0 & \alpha_h & 0 & 0 & 3\alpha_m & a_{Na(6)} & 2\beta_m & 0 \\ 0 & 0 & \alpha_h & 0 & 0 & 2\alpha_m & a_{Na(7)} & 3\beta_m \\ 0 & 0 & 0 & \alpha_h & 0 & 0 & \alpha_m & a_{Na(8)} \end{pmatrix} \tag{16}$$

$$A_K = \begin{pmatrix} a_{K(1)} & \beta_n & 0 & 0 & 0 \\ 4\alpha_n & a_{K(2)} & 2\beta_n & 0 & 0 \\ 0 & 3\alpha_n & a_{K(3)} & 3\beta_n & 0 \\ 0 & 0 & 2\alpha_n & a_{K(4)} & 4\beta_n \\ 0 & 0 & 0 & \alpha_n & a_{K(5)} \end{pmatrix}. \tag{17}$$

In equations (16) and (17), the diagonal elements are given by

$$a_{Na}(i) = -\sum_{j\neq i}^{8} A_{Na}(j, i),$$

$$a_K(i) = -\sum_{j\neq i}^{5} A_K(j, i).$$

Here the non-diagonal elements $A_{Na}(j, i)$ or $A_{Na}(j, i)$ denote the $j \rightarrow i$ transition rates.

Given the normalization constraint of the channel-state fractions, the dimensions of the transition matrices can be reduced by 1. In the model, one typically keeps the numbers of both the Na^+ and K^+ channels fixed with the number of the Na^+ channel three times as big as that of the K^+ channel. By changing the membrane area, both the sodium and potassium channel numbers are changed. Thus, if not specified otherwise, we denote the K^+ channel number by N in the following, and the corresponding Na^+ channel number is then given by $3N$.

3. Master equations and stochastic simulation algorithms

The gating behavior of ion channels is subject to microscopic fluctuations producing random changes in the ion current (channel noise). This noise originates from fluctuations in the gating transition because of the discrete molecule numbers and becomes more influential when the number of particles is small. Since smaller extensions of action potential–carrying membranes decrease the number of ion channels per axonal length, miniaturization of neuronal structures comes with the disadvantage of larger noise. With channel densities of a few tens per μm^2, Faisal, White and Laughlin found a lower limit of 0.1 μm axonal diameter for reliable transmission of membrane potentials [11, 63]. Furthermore, noise becomes significant at diameters of 0.5 μm and less. Analysis of anatomical data showed that many neurons from the cortex or cerebellum are in fact in this fluctuation range [11].

For small channel numbers, the standard representation of chemical reactions, namely the differential equations based on the law of mass action, need to be replaced by the corresponding master equations, where the reactions or gating transitions are treated as Markovian birth-death processes. As an example, we consider the evolution of a number of subunits that transition between two configurations (active and inactive) with rates of activation and inactivation α_w and β_w as above. Taking k to be the number of subunits in the open or active state and N the total number of subunits, we obtain as a master equation:

$$\begin{aligned} \frac{dP(k, t)}{dt} &= \alpha_w((N - k + 1)P(k - 1, t) \\ &\quad - (N - k)P(k, t)) \\ &\quad + \beta_w((k + 1)P(k + 1, t) - kP(k, t)), \end{aligned} \tag{18}$$

where $P(k, t)$ is the probability of having k subunits in the open state at time t.

While master equations can be solved for simple cases in an analytical way, this is not practical in the case of more complex master equations, involving many channels or many different receptor states. For instance, for a subunit-based model with three types of binding sites, we need to determine the evolution of a probability $P(k_m, k_h, k_n, t)$ in a three-dimensional occupation number space. For the channel-based model, the probability in an even larger space must be tracked. In this case, solutions can be obtained by Monte Carlo methods, where exemplary trajectories are calculated using random numbers in a way appropriate to the transition rates. Single trajectories can then be collected to obtain statistical features of the system.

A foundation of stochastic simulation algorithms was given by Gillespie [52, 53]. The approach is based on the notion of a propensity a_i for each possible transition or reaction R_i. Then

$$a_i \mathrm{d}t = h_i c_i \mathrm{d}t \tag{19}$$

is the probability that reaction R_i occurs during the next infinitesimal time step dt. Here c_i denotes the reaction constant of R_i (the probability density that a combination of molecules reacts) and h_i is the number of particle combinations of that particular reaction. For instance, in the case of a mono-molecular reaction, $A \rightarrow B$, h equals X_A, where X_A is the number of A-molecules in a certain well-mixed volume V, and c equals the macroscopic rate k of the transition. Similarly, for $A + B \rightarrow 2A$, $h = X_A X_B$ and the macroscopic $k = cV$. If a reaction is called, the corresponding numbers of participating molecule species, X_j, $j = 1, ..., K$, are updated according to the stoichiometric factors, which are conveniently placed into a matrix, ν_{ij}, defined as

$$\nu_{ij} \equiv \text{change in the number of } X_j \text{ molecules produced by one } R_i \text{ reaction.} \tag{20}$$

Using the stoichiometric factors one can write the general form of the chemical master equation for the probability $P(\boldsymbol{x}, t)$ as

$$\frac{\partial}{\partial t} P(\boldsymbol{x}, t) = \sum_j a_j(\boldsymbol{x} - \boldsymbol{\nu}_j) P(\boldsymbol{x} - \boldsymbol{\nu}_j, t) - a_j(\boldsymbol{x}) P(\boldsymbol{x}, t). \tag{21}$$

Here $\boldsymbol{x}$ is the vector of occupation numbers for X_j and $\boldsymbol{\nu}_i = (\nu_{ij})_j$.

The stochastic algorithm determines the time of the next reaction and which reaction it will be, given the state $\boldsymbol{X} = (X_A, X_B, ...)$ at the starting time t. Let $P_0(\tau)$ be the probability that no reaction will occur in $(t, t + \tau)$ and $a_i = a_i(\boldsymbol{X})$ the propensity at time t. Since $1 - \sum_i a_i \mathrm{d}\tau$ is the probability that no reaction will occur in dτ, where the sum's index runs over all reactions, we find that

$$P_0(\tau + \mathrm{d}\tau) = P_0(\tau)\left(1 - \sum_i a_i \mathrm{d}\tau\right) \tag{22}$$

is the probability that no reaction has occurred in $(t, t + \tau + \mathrm{d}\tau)$. The last equation implies that $P_0(\tau) = \exp(-\sum_i a_i \tau)$. On the other hand, the probability that the next reaction is R_i and it occurs in $(t + \tau, t + \tau + \mathrm{d}t)$ is $P(\tau, i)\mathrm{d}t = P_0(\tau) a_i \mathrm{d}t$, i.e.,

$$P(\tau, i) = a_i \exp\left(-a_0 \tau\right), \tag{23}$$

where $a_0 = \sum_i a_i$ is the sum of all propensities. The probability density $P(\tau, i)$ can be implemented by drawing two random numbers r_1 and r_2 from a uniform distribution in the interval [0, 1], and choosing τ and i such that

$$a_0 \cdot \tau = \ln\left(1/r_1\right), \qquad \sum_{j=1}^{i} a_j \leqslant a_0 \cdot r_2 < \sum_{j=1}^{i+1} a_j. \tag{24}$$

In this way, the next event to occur is R_i and it will occur after time τ. This method is the so-called direct method [52]. Variants, which differ in the application of random numbers, are the first [52] and next reaction methods [64].

The method described above allows us to obtain exact solutions of the chemical master equations. A simpler method, sufficiently accurate for many circumstances and also used in discrete simulations below, is to choose a small time step τ and then use the propensities as a conditional probability for each transition during a time step τ.

4. Langevin approaches

4.1. General remarks on the chemical Langevin equations

In many systems the number of different reactions is so large that simulation with the stochastic algorithm described above is computationally demanding. For example, a single axonal membrane patch may contain several thousand channels of different types and with complex gating schemes [57]. Under those conditions, solution of the master equation in an exact way, i.e., by considering all discrete transitions, is inefficient because the number of required random numbers scales with the number of channels. To overcome this problem, several reduced stochastic approaches have been developed. The following outline, leading to approximate stochastic differential equations, focuses on the derivation of the chemical Langevin equations put forward by Gillespie and emphasizes the relation to propensities discussed above as well as computer simulation methods. In the limit of large channel numbers one recovers the reaction rate equations discussed in section 2. Relations of Gillespie's derivation to the asymptotic expansions are discussed in [65].

We begin with a brief discussion of the τ-leap method. τ-leaping allows the collective execution of several instances of each reaction during one time step of length τ [66]. Here τ must satisfy the following condition:

(i) τ is small enough so that no propensity changes substantially during this time (leap condition),

i.e. the reaction channels decouple at this time scale. The number of realizations of reaction R_i during time τ is then given by the Poisson distribution

$$P_{a_i \tau}(k) = \frac{(a_i \tau)^k}{k!} \mathrm{e}^{-a_i \tau}.$$

The method is numerically efficient only if τ can be chosen relatively large, so that the number of drawings of random numbers can be kept small.

If changes in occupation number during a time step τ are large, the Poisson distribution can be approximated by a Gaussian distribution for the number of realizations:

$$G(a_i\tau,\, a_i\tau) = a_i\tau + \sqrt{a_i\tau}\,G(0,\,1), \tag{25}$$

where $G(m,\, v)$ describes a Gaussian variable with mean m and variance v.

It follows that under the condition (i) and if, additionally,

(ii) τ is large enough so that any reaction occurs multiple times during each time step τ,

the evolution can be approximated by using the Gaussian distribution instead of the Poisson distribution [67]. This effectively means that the evolution law can be written in the form

$$X_j(t+\tau) = X_j(t) + \sum_i \nu_{ij} a_i \tau + \sum_i \nu_{ij}\sqrt{a_i\tau}\,\xi_i, \tag{26}$$

where ξ_i denotes Gaussian variables with zero mean and unit variance. For small τ, a stochastic differential equation is obtained that corresponds to the Langevin equation for random walks but with state-dependent steps.

The conditions (i) and (ii) may be conflicting. This happens particularly if a single step of one reaction causes large changes in the propensity of another reaction. The value of τ must be small enough to accommodate the leap condition (i) for the second reaction. However, then condition (ii) may not hold for the first reaction and its number change cannot be approximated by a Gaussian distribution. If both conditions (i) and (ii) hold, and the product $a_i\tau$ becomes large, the noise term in the chemical Langevin equation is small compared to the deterministic term and it can be neglected. In those circumstances, we recover the deterministic reaction rate law.

The Langevin equation (26) as derived by Gillespie requires one Gaussian process per reaction channel. Depending on the specific Markov chain, or more precisely, the form of the stoichiometric matrix ν, the number of independent stochastic terms can be reduced [68] and the form of the noise terms is not unique. An equivalent Langevin equation can be obtained by using one independent stochastic process per reversible reaction. In the case of the activation and inactivation of subunits, equation (26) requires two random processes, but those two entries can be replaced with one entry combining the two noise amplitudes (see equation (30)). A more complex application of this reformulation occurs for the case of channel-based models in section 4.3.

An alternative derivation of the chemical Langevin equation is based on the Kramers–Moyal expansion. Here one expands the function $f_j(\boldsymbol{x}) = a_j(\boldsymbol{x})P(\boldsymbol{x},\, t)$ in $\boldsymbol{x}$ for small jumps $\boldsymbol{\nu}_j$. Inserting in the master equation (21) and truncating the expansion after the second order yields the Fokker–Planck equation

$$\frac{\partial P(\boldsymbol{x},\, t)}{\partial t} = -\sum_j^K \nu_{jk}\frac{\partial}{\partial x_k} a_j(\boldsymbol{x})P(\boldsymbol{x},\, t) + \frac{1}{2}\sum_j^K \nu_{jk}\nu_{jl}\frac{\partial}{\partial x_k}\frac{\partial}{\partial x_l} a_j(\boldsymbol{x})P(\boldsymbol{x},\, t). \tag{27}$$

This equation corresponds to a set of Langevin equations

$$\frac{\mathrm{d}X_i(t)}{\mathrm{d}t} = \sum_j \nu_{ji} a_j(\boldsymbol{X}(t)) + \sum_j \nu_{ji}\sqrt{a_j(\boldsymbol{X}(t))}\,\Gamma_j(t), \quad i = 1,\ldots,K \tag{28}$$

where the $\Gamma_j(t)$ are Gaussian white noises with zero mean and unit variance [67, 69]. These equations equivalent to those of equation (26).

Several authors have studied the behavior of solutions to the Fokker–Planck equation for bistable systems and found substantial differences to the solutions of the original master equation [70, 71]. Most importantly, this difference persists even for the case of very large particle numbers. It is interesting to think about the breakdown of the continuous approximation in this case in terms of the two conditions posed by Gillespie. However, a detailed discussion of this issue would be out of the scope of this review, where instead we focus on the case of approximation errors for small and intermediate channel numbers and how they are related to multiple noise sources from subunit and channel transitions.

4.2. Subunit-based LA

The gate-kinetic Langevin approach (subunit-based LA) was first suggested by Fox and Lu in the Hodgkin–Huxley neuron model [15, 20]. In the subunit-based LA, the source of internal channel noise is supposed to be the stochastic gating of channel subunits. Because it is easy to implement and computationally efficient, the subunit-based LA was widely used as an approximation for stochastic HH channel dynamics [55, 57–59, 72–74] and other channel systems [39, 40, 75]. Note that the subunit open fraction may be out of the range of [0, 1] due to the addition of Gaussian noise, especially at small channel number. In order to ensure a fraction in the unit interval, a simple cut-off procedure is applied to set the subunit fraction at 0 or 1 when the fraction becomes smaller than zero or larger than 1.

4.2.1. Identical subunits

a. Fox–Lu's subunit-based LA. In this approach, subunits of the same type are identical, implying that subunit open fractions can be calculated by averaging across all subunits with the same type. Thus, the stochastic version of deterministic subunit-based expression in equation (5) can be rewritten [15, 20]:

$$\frac{dw}{dt} = \alpha_w(1-w) - \beta_w w + \sigma_w \xi_w(t), \quad (w = m, h, \text{ or } n), \tag{29}$$

where $\xi_w(t)$ is a Gaussian white noise with zero mean and unit variance, and σ_w denotes the intensity of the noise and satisfies the equation

$$\sigma_w = \sqrt{\frac{\alpha_w(1-w) + \beta_w}{N_i}}, \tag{30}$$

where N_i denotes the count of Na^+ or K^+ ion channels.

With respect to the HH neuron model, it has been shown that the subunit LA underestimated channel noise for the subunit LA [55–57, 76]. As a result, the subunit LA should be modified to give a better statistical result.

b. Rounding of the open channel number. Rubinstein *et al* first reported that the Fox–Lu subunit LA produced different action potential statistics (including the firing efficiency and mean latency for the neuron responding to a monophasic pulse) from the Markov method for simulations with 1,000 Na^+ channels [76]. They suggested that the number of the open Na^+ channels should be rounded down to the nearest integer so as to be consistent with the integer values produced by the Markov method. Later, Bruce argued that a rounding algorithm to the nearest integer for the number of open Na^+ channels could improve the accuracy of the Fox–Lu subunit LA [55].

When responding to a monophasic pulse, the initiation of an action potential in the HH model is highly dependent on the number of open Na^+ channels and consequently may be sensitive to any rounding of the open Na^+ channels' number. In detail, compared to the rounding algorithm to the nearest integer, the rounding down treatment always underestimates the number of open Na^+ channels which causes a current to trigger the action potential. Even with 1,000 Na^+ channels, the accumulation of small neglected quantities can lead to a statistical difference. As a result, the rounding down treatment may produce a decrease in firing efficiency and an increase in the spike latency.

c. Rescaled noise intensity. Because the subunit LA underestimates the channel noise, a simple idea is then to rescale the noise intensity added to the subunit fraction [77]. By rescaling the noise intensity with an empirical factor, equation (30) will become

$$\sigma_w = \lambda_w \sqrt{\frac{\alpha_w(1-w) + \beta_w}{N_i}} \tag{31}$$

where the constant λ_w is used to rescale the noise intensity.

Huang *et al* first discussed the rescaled subunit-based LA for localized intracellular calcium signals (Ca^{2+} puffs) released from a cluster of IP_3Rs in the ER membrane [78]. Because a larger mean Ca^{2+} concentration is obtained with the identical subunit LA than that with Markov method, indicating an overestimation of channel noise, a factor of $\lambda = 0.7$ has been suggested [78] for stochastic IP_3R channel noise. The rescaled subunit LA can reproduce the mean Ca^{2+} concentration even at a channel number around 10.

4.2.2. Independent subunits

For the identical subunit-based LA, subunits of K^+ channel and Na^+ channel of the same type are disturbed by identical Gaussian noise. Actually, subunits in a channel are independent, implying that each subunit has distinct contribution to the open fractions of the ion channel. For example, the subunits in a K^+ channel can be distinguished by n_1, n_2, n_3 and n_4. For the Na^+ channel a similar consideration follows. As a result, ion-channel open fractions can be expressed by $\rho_{Na} = m_1 m_2 m_3 h_1$ and $\rho_K = n_1 n_2 n_3 n_4$ and each subunit can be disturbed by a different Gaussian noise.

This approach was first mentioned in [40] to discuss the stochastic IP_3R channel dynamics to release Ca^{2+} puffs. Later, Huang *et al* and Goldwyn *et al* implemented it [58, 78] in calcium and neuron models, respectively. Although the consideration of independent subunits is biologically more realistic, for the stochastic HH neuronal model Goldwyn *et al* indicated that independent subunit LA gives worse action potential statistics than the identical subunit LA [58].

4.3. Channel-based LA with standard diffusion matrix

In recent years there have been a number of publications that aim at derivation and simulation of channel-based Langevin equations [58, 60–62, 79–84]. The channel-based LA was already described by Fox and Lu using the system size expansion [15]; however, the resulting scheme was not implemented until very recently by Goldwyn *et al* [58]. We discuss the implementation by Goldwyn *et al* [58], which is based on a numerical calculation of the matrix square root needed for the Fox and Lu channel-based LA. We also discuss the issues of the boundedness of state fractions [62], and the discretization of open channel numbers [81].

Despite the possibility of such a straightforward and accurate noise representation, there remains the problem that in the channel-based approach the number of equations is much larger than in the subunit-based approach. In a different method, several researchers have tried to preserve the original deterministic HH equation structure, but including an effective noise from the channel-based description. This

noise is then added to the deterministic channel fraction within the voltage equation. For this line of incorporating channel noise, we here discuss the approaches by Linaro *et al* [79], and Güler [82].

4.3.1. Channel-based LA with unbounded state fractions a. Quasistationary approach (*original Fox–Lu LA*). To consider the channel noise together with the deterministic channel-based HH model, the evolution of channel state fractions can be traced by the following stochastic HH differential equations [15, 20]

$$\frac{\mathrm{d}\mathbf{Y}}{\mathrm{d}t} = A_{\mathrm{Na}}\mathbf{Y} + S_{\mathrm{Na}}\xi_{\mathrm{Na}}, \tag{32}$$

$$\frac{\mathrm{d}\mathbf{X}}{\mathrm{d}t} = A_{\mathrm{K}}\mathbf{X} + S_{\mathrm{K}}\xi_{\mathrm{K}}, \tag{33}$$

where ξ_{Na} and ξ_{K} are noise vectors with each element a Gaussian white noise with zero means and unit variances. The values of S_{Na} and S_{K} are the matrix square roots of diffusion matrices D_{Na} and D_{K}, respectively, which depend on the state variables and the voltage-dependent subunit opening and closing rates.

The diffusion matrices D_{Na} and D_{K} are given as follows:

$$D_{\mathrm{Na}} = \frac{1}{N_{\mathrm{Na}}} \begin{pmatrix} d_{\mathrm{Na}}(1) & -\left(3\alpha_m y_{00} + \beta_m y_{10}\right) \\ -\left(3\alpha_m y_{00} + \beta_m y_{10}\right) & d_{\mathrm{Na}}(2) \\ 0 & -2\left(\alpha_m y_{10} + \beta_m y_{20}\right) \\ 0 & 0 \\ -\left(\alpha_h y_{00} + \beta_h y_{01}\right) & 0 \\ 0 & -\left(\alpha_h y_{10} + \beta_h y_{11}\right) \\ 0 & 0 \\ 0 & 0 \\ 0 & 0 \\ -2\left(\alpha_m y_{10} + \beta_m y_{20}\right) & 0 \\ d_{\mathrm{Na}}(3) & -\left(\alpha_m y_{20} + 3\beta_m y_{30}\right) \\ -\left(\alpha_m y_{20} + \beta_m y_{30}\right) & d_{\mathrm{Na}}(4) \\ 0 & 0 \\ 0 & 0 \\ -\left(\alpha_h y_{20} + \beta_h y_{21}\right) & 0 \\ 0 & -\left(\alpha_h y_{30} + \beta_h y_{31}\right) \\ -\left(\alpha_h y_{00} + \beta_h y_{01}\right) & 0 \\ 0 & -\left(\alpha_h y_{10} + \beta_h y_{11}\right) \\ 0 & 0 \\ 0 & 0 \\ d_{\mathrm{Na}}(5) & -\left(3\alpha_m y_{01} + \beta_m y_{11}\right) \\ -\left(3\alpha_m y_{01} + \beta_m y_{11}\right) & d_{\mathrm{Na}}(6) \\ 0 & -2\left(\alpha_m y_{11} + \beta_m y_{21}\right) \\ 0 & 0 \\ 0 & 0 \\ 0 & 0 \\ -\left(\alpha_h y_{20} + \beta_h y_{21}\right) & 0 \\ 0 & -\left(\alpha_h y_{30} + \beta_h y_{31}\right) \\ 0 & 0 \\ -2\left(\alpha_m y_{11} + \beta_m y_{21}\right) & 0 \\ d_{\mathrm{Na}}(7) & -\left(\alpha_m y_{21} + 3\beta_m y_{31}\right) \\ -\left(\alpha_m y_{21} + 3\beta_m y_{31}\right) & d_{\mathrm{Na}}(8) \end{pmatrix} \tag{34}$$

$$D_{\mathrm{K}} = \frac{1}{N_{\mathrm{K}}} \begin{pmatrix} d_{\mathrm{K}}(1) & -\left(4\alpha_n x_0 + \beta_n x_1\right) \\ -\left(4\alpha_n x_0 + \beta_n x_1\right) & d_{\mathrm{K}}(2) \\ 0 & -\left(3\alpha_n x_1 + 2\beta_n x_2\right) \\ 0 & 0 \\ 0 & 0 \\ 0 & 0 \\ -\left(3\alpha_n x_1 + 2\beta_n x_2\right) & 0 \\ d_{\mathrm{K}}(3) & -\left(2\alpha_n x_2 + 3\beta_n x_3\right) \\ -\left(2\alpha_n x_2 + 3\beta_n x_3\right) & d_{\mathrm{K}}(4) \\ 0 & -\left(\alpha_n x_2 + 4\beta_n x_4\right) \\ 0 & 0 \\ 0 & 0 \\ 0 & 0 \\ -\left(\alpha_n x_2 + 4\beta_n x_4\right) & 0 \\ d_{\mathrm{K}}(5) & -\left(3\alpha_n x_3 + 3\beta_n x_4\right) \\ -\left(3\alpha_n x_3 + 3\beta_n x_4\right) & d_{\mathrm{K}}(6) \end{pmatrix} \tag{35}$$

For D_{Na} and D_{K} in equations (34) and (35), the diagonal elements are given by

$$d_{\mathrm{Na}}(i) = -\sum_{j\neq i}^{8} D_{\mathrm{Na}}(j,\, i)$$

$$d_{\mathrm{K}}(i) = -\sum_{j\neq i}^{5} D_{\mathrm{K}}(j,\, i).$$

Due to the Gaussian noise terms added, channel state fractions are no longer guaranteed to lie on the bounded domain, but have a probability of violating the meaningful interval [0,1]. Since Goldwyn *et al* allow for simplicity that fractions evolve unboundedly, for values outside [0,1] the positive-semidefiniteness of diffusion matrices may not be given thus hindering the computations of the matrix square roots. For the implementation of this model, the use of equilibrium values of channel state fractions (see equations (36) and (37) for each given time-depending voltage V) was therefore suggested in [58], and is known as the quasistationary model. However, using this approximation, the mean period of interspike interval at large channel number is significantly underestimated. This problem has been reported in [60, 62].

$$\overline{x}_i = \binom{4}{i} \frac{\alpha_n^i \beta_n^{4-i}}{\left(\alpha_n + \beta_n\right)^4} \tag{36}$$

$$\overline{y}_{jk} = \binom{3}{j} \frac{\alpha_m^j \beta_m^{3-j} \alpha_h^k \beta_h^{1-k}}{\left(\alpha_m + \beta_m\right)^3 \left(\alpha_h + \beta_h\right)} \tag{37}$$

b. Orio et al approach (*Orio LA*). Orio *et al* proposed a simple structure of the square root matrices to solve the stochastic HH differential equations:

$$\frac{\mathrm{d}\mathbf{Y}}{\mathrm{d}t} = A_{\mathrm{Na}}\mathbf{Y} + S_{\mathrm{Na}}^{\mathrm{Orio}}\xi_{\mathrm{Na}}, \tag{38}$$

$$\frac{\mathrm{d}\mathbf{X}}{\mathrm{d}t} = A_{\mathrm{K}}\mathbf{X} + S_{\mathrm{K}}^{\mathrm{Orio}}\xi_{\mathrm{K}}. \tag{39}$$

In this approach, the Cholesky decomposition was extended to solve the stochastic terms of complex kinetic schemes, such as the 8-state sodium channel. For instance, the random term for i is equal to the square root of the sum of the forward ($i \to j$) and backward ($i \leftarrow j$) transition probabilities for the transition pair $i \leftrightarrows j$, scaled by the inverse of the channel number. The square root in the square root matrices $S_{\mathrm{Na}}^{\mathrm{Orio}}$ and $S_{\mathrm{K}}^{\mathrm{Orio}}$ in equations (38) and (39) was applied to the absolute value of the argument.

As a consequence, the channel-state fractions are free to evolve without any approximation to the diffusion matrices [60]:

$$S_{\mathrm{Na}}^{\mathrm{Orio}} = \begin{pmatrix} 1 & 0 & 0 & 1 & 0 \\ -1 & 1 & 0 & 0 & 1 \\ 0 & -1 & 1 & 0 & 0 \\ 0 & 0 & -1 & 0 & 0 \\ 0 & 0 & 0 & -1 & 0 \\ 0 & 0 & 0 & 0 & -1 \\ 0 & 0 & 0 & 0 & 0 \\ 0 & 0 & 0 & 0 & 0 \end{pmatrix} \begin{pmatrix} 0 & 0 & 0 & 0 & 0 \\ 0 & 0 & 0 & 0 & 0 \\ 1 & 0 & 0 & 0 & 0 \\ 0 & 1 & 0 & 0 & 0 \\ 0 & 0 & 1 & 0 & 0 \\ 0 & 0 & -1 & 1 & 0 \\ -1 & 0 & 0 & -1 & 1 \\ 0 & -1 & 0 & 0 & -1 \end{pmatrix} \frac{\mathbf{F}_{\mathrm{Na}}}{\sqrt{N_{\mathrm{Na}}}} \tag{40}$$

$$S_{\mathrm{K}}^{\mathrm{Orio}} = \begin{pmatrix} 1 & 0 & 0 & 0 \\ -1 & 1 & 0 & 0 \\ 0 & -1 & 1 & 0 \\ 0 & 0 & -1 & 1 \\ 0 & 0 & 0 & -1 \end{pmatrix} \frac{\mathbf{F}_{\mathrm{K}}}{\sqrt{N_{\mathrm{K}}}}, \tag{41}$$

where $\mathbf{F}_{\mathrm{Na}}$ and $\mathbf{F}_{\mathrm{K}}$ are 10×10 and 4×4 diagonal matrices and their elements on the diagonal are

$$\begin{pmatrix} \sqrt{3\alpha_m y_{00} + \beta_m y_{10}} \\ \sqrt{2\alpha_m y_{10} + 2\beta_m y_{20}} \\ \sqrt{\alpha_m y_{20} + 3\beta_m y_{30}} \\ \sqrt{\alpha_h y_{00} + \beta_h y_{01}} \\ \sqrt{\alpha_h y_{10} + \beta_h y_{11}} \\ \sqrt{\alpha_h y_{20} + \beta_h y_{21}} \\ \sqrt{\alpha_h y_{30} + \beta_h y_{31}} \\ \sqrt{3\alpha_m y_{01} + \beta_m y_{11}} \\ \sqrt{2\alpha_m y_{11} + 2\beta_m y_{21}} \\ \sqrt{\alpha_m y_{21} + 3\beta_m y_{31}} \end{pmatrix}$$

and

$$\begin{pmatrix} \sqrt{4\alpha_n x_0 + \beta_n x_1} \\ \sqrt{3\alpha_n x_1 + 2\beta_n x_2} \\ \sqrt{2\alpha_n x_2 + 3\beta_n x_3} \\ \sqrt{\alpha_n x_3 + 4\beta_n x_4} \end{pmatrix}$$

respectively.

Instead of the five and eight random terms in equations (35) and (34) suggested by Fox and Lu [20] and implemented by Goldwyn *et al* [58] for K^+ and Na^+ channels, the simplified formulations proposed by Orio *et al* require four and ten random terms, respectively. Although one more random term is added, the expensive matrix operations are avoided, greatly reducing the total computational cost during the numerical simulation [84]. Such a simpler expression for the diffusion matrix results with the fulfillment of $SS^T = D$.

4.3.2. Channel-based LA with bounded state fractions

Both the quasi-stationary approach and the Orio approach do not consider any bounding procedure to limit the channel state fraction between 0 and 1. When the number of channels is sufficiently large, the unbounded approaches are able to reproduce a quantitatively accurate approximation to the exact Markovian chain simulation, such as the mean and variance of the open fractions [58, 60]. It seems that the effect of the free boundary is only relevant at small channel number due to the large Gaussian noise. For instance, as illustrated in figure 2, two typical spikes are generated by the original unbounded Fox–Lu approach with the number of K^+ channel equal to 10. Instead of inhibiting the spiking, the negative open fraction of the K^+ channel at the initial stage of spiking might trigger a spiking or an overly depolarized phase.

However, even at large channel number, the Gaussian noise can frequently drive the open fraction to be negative. At large channel number without stimulus, the channel noise becomes weak and the HH channel frequently stays at the quiet state. Thus the open

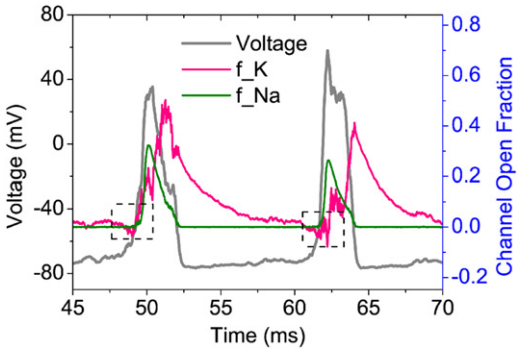

Figure 2. Trajectory of voltage (gray) as well as open fractions of potassium (pink) and sodium (green) channels. The channel number is 10. Here the stimulus current $I_{\text{stim}} = 0$.

fractions of Na^+ and K^+ channels should often reside at zero. As a result, even a small Gaussian noise can easily drive the open fractions to become negative. The probability of negative channel-state fractions still remains high (about 10%) even at $N = 5000$, especially for Na^+ channels [62]. One may argue that such a small negative open probability could induce little effect on stochastic action potentials. However, simulation results showed that suitable probability-bounded LA can improve the stochastic simulation substantially. In the following, we discuss several numerical algorithms applied to the original master-equation LA, aiming at solving the boundary problem.

a. Simply bounded approaches. The overflowing part of any channel state fraction can be simply truncated and then those coupled and truncated state fractions are normalized again so as to ensure persistent satisfaction of the normalization constraint, $\Sigma_{j,K=0,0}^{3,1} y_{j,k} = 1.0$ for Na^+ channels and $\Sigma_{i=0}^{4} x_i = 1.0$ for K^+ channels. However, as pointed by Huang *et al* [62], this simple truncated scheme could not reproduce the channel noise correctly for $N < 2000$, requiring better bounded schemes. Alternatively, one can ignore the large noise and retry new noise terms in one simulation step until the boundary condition is satisfied eventually [85]. In fact, applying a small noise just means to generate an uncorrect channel noise in the model, similar to the simple truncated scheme. This scheme would also greatly slow down the speed at small channel number.

b. Reflecting approach (*reflected LA*). A reflected scheme was first applied to limit the neuron channel state fractions within the biologically meaningful ranges through incorporating the reflecting process with an orthogonal projection method into the evolutions of SDEs [61]. The approach adds reflecting processes R_{Na} and R_{K} to the stochastic differential equations to deal with the behavior of the open fractions $\mathbf{Y}$ and $\mathbf{X}$ on the boundary. Such a reflecting process is a minimal procedure which forces the open fraction to remain in the interval [0, 1] [61]. Mathematically, it computes the projection of a vector onto the canonical simplex which satisfies the condition of the open fraction in [0,1] and ensures that their sum equals a unit [86]. The numerical expressions are given by

$$\begin{aligned}\mathbf{Y}(t+\Delta t) &= \mathbf{Y}(t) + A_{\text{Na}}\mathbf{Y}(t)\Delta t \\ &+ \frac{1}{\sqrt{\Delta N_{\text{Na}}}} L_{\text{Na}} J_{\text{Na}} \xi_{\text{Na}}(t)\sqrt{\Delta t} \\ &+ \Delta R_{\text{Na}}(t),\end{aligned} \tag{42}$$

$$\begin{aligned}\mathbf{X}(t+\Delta t) &= \mathbf{X}(t) + A_{\text{K}}\mathbf{X}(t)\Delta t \\ &+ \frac{1}{\sqrt{\Delta N_{\text{K}}}} L_{\text{K}} J_{\text{K}} \xi_{\text{K}}(t)\sqrt{\Delta t} + \Delta R_{\text{K}}(t),\end{aligned} \tag{43}$$

where the reflecting processes R_{Na} and R_{K} can be found in [61].

The production of L_{K} and J_{K} or L_{Na} and J_{Na} is the alternative representation of the square root matrix S_{K} or S_{Na}. In fact, the square root matrices are non-unique, i.e. there are different matrices S such that $SS^T = D$. In [68] it was shown how the matrices S can be explicitly chosen to allow an efficient numerical implementation that does not require the time-consuming matrix square root calculation. A particular choice for S_{Na} and S_{K} is given by $\frac{L_{\text{Na}} J_{\text{Na}}}{\sqrt{\Delta N_{\text{Na}}}}$ and $\frac{L_{\text{K}} J_{\text{K}}}{\sqrt{\Delta N_{\text{K}}}}$ respectively. The matrices L_{Na}, J_{Na}, L_{K}, and J_{K} are provided in [61]. It was pointed out and will also be shown below that the efficiency of channel-based LA can be significantly enhanced with these noise term representations [61, 62, 81].

The action potential statistics, including the mean action potential, the mean spike amplitude and the mean interspike interval from simulations of ion-channel dynamics using the reflected SDE have been compared with those derived from the discrete-state Markov method [62]. It has been shown that the reflected approach is invalid below the channel number of 500 [61, 62, 84]. This is mainly because the reflecting method actually applies smaller noise by ignoring the extra open fraction out of [0, 1] with a projection process.

c. Truncated and restored approach (*truncated-restored LA*). The failure of the reflected LA may be partly due to simply throwing away the non-meaningful state fractions after the reflecting procedure. Huang *et al* demonstrated that the restoration after a bounded operation is an essential step, which puts the changes of the channel state fractions after a bounded process back to the SDEs at the next simulation step [62]. Taking K^+ channels for an example, the vector $\mathbf{E}(t)$ is truncated from $\mathbf{X}$ at time t and then added to the SDEs at the next time step $t + \Delta t$ to get a temporary vector $\mathbf{K}(t + \Delta t)$. Once again, the bounded process is executed to get the truncated vector $\mathbf{E}(t + \Delta t)$. As a result, the two continuous restoration steps define the following two vector equations:

$$\mathbf{K}(t+\Delta t) = \mathbf{X}(t) + A_K\mathbf{X}(t)\Delta t + S_K\xi_K(t)\sqrt{\Delta t} + \mathbf{E}(t), \tag{44}$$

$$\mathbf{X}(t+\Delta t) = \mathbf{K}(t+\Delta t) - \mathbf{E}(t+\Delta t), \tag{45}$$

Putting equations (44) and (45) together, the iteration equations can be expressed as:

$$\mathbf{X}(t+\Delta t) = \mathbf{X}(t) + A_K\mathbf{X}(t)\Delta t + \left(S_K\xi_K(t) + \eta_K(t)\right)\sqrt{\Delta t}, \tag{46}$$

$$\eta_K(t)) = \frac{(\mathbf{E}(t+\Delta t) - \mathbf{E}(t))}{\sqrt{\Delta t}}, \tag{47}$$

where the vector $\eta_K(t)) = \{\varphi_i(t)\}$ with elements $\{\varphi_i(t)$ $(i = 0, 1, 2, 3, 4)$. The truncated vector $\eta_{Na}(t)) = \{\psi_{j,k}(t)\}$ corresponding to Na^+ channels can also be defined in a similar way. The reason why the restoration process is indispensable for a bounded method is that it maintains the mean of the state fractions derived analytically from the channel-based Fox–Lu approach in [58]. For example, after two continuous simulation steps, the bounded state fraction is $\mathbf{X}(t+\Delta t) + \mathbf{E}(t) - \mathbf{E}(t+\delta t)$. As a result, the average of the state fraction can be reformulated to be $\langle\mathbf{X}(t+\Delta t)\rangle + \langle\mathbf{E}(t)\rangle - \langle\mathbf{E}(t+\delta t)\rangle$, where $\langle\mathbf{E}(t)\rangle = \langle\mathbf{E}(t+\delta t)\rangle$. By comparison of the action potential statistics, including the mean action potential, the mean spike amplitude and the mean interspike interval, the truncated and restored LA show a good agreement with the Markov method even at the channel number about 100.

Combining the restored process with the reflected approach, the simulation accuracy is as good as the truncated and restored LA [62]. Thus, the failure of the reflected approach in [61] occurs because the reflection process simply throws away the extra values of the state fractions. However, with the restoration process to put the truncated fractions back into the state fractions in the next time step [62], one can accurately preserve the strength of the Gaussian noise for channel stochasticity. Another conclusion is that after considering the restoration of the truncated noise, a time-correlated colored noise is introduced in the simulation method [62].

4.3.3. Channel-based LA with discretized open fraction

Typically, the Langevin approaches could not accurately replicate the properties of the Markov model at small channel number. However, an effective continuous-to-discrete treatment was proposed in [81] in order to capture the discrete behavior of the channel open fraction especially for small membrane patch areas. Assuming that $x_4(t)$ is the channel open fraction at time t, then the integer number of the open channel derived from x_4 has two possibilities: one is the maximal integer $N_{K,open-}$ that is smaller than x_4N_K and the other is the minimal integer $N_{K,open+}$ that is bigger than x_4N_K. Thus, a parameter θ_K is proposed to define the propensity to the two cases. As a result, if

$$x_4N_K < \left(N_{K,open-} + \theta_K\right), \tag{48}$$

one sets

$$\rho_K = N_{K,open-}, \tag{49}$$

and, otherwise,

$$\rho_K = N_{K,open+}. \tag{50}$$

From the calculations of the mean and standard deviation of the open fractions of Na^+ channels, Huang *et al* found that the open fraction of Na^+ channels is sensitive to parameter θ_{Na}, thus it is of importance for the Na^+ channel to choose a proper θ_{Na} with respect to the adopted continuous LA. As suggested in [81], the optimal choice is for K^+ channels, $\theta_K = 0.5$, while for Na^+ channels, $\theta_{Na} = 0.4$. It has been shown that at small channel number the discretization procedure can better mimic the trigger behavior of the stochastic channel dynamics, giving an improved stochastic description [81]. Rubinstein *et al* and Bruce previously suggested different rounding methods with subunit-based LA [55, 76], which are actually special cases of this discrete method.

4.4. Channel-based LAs with effectively colored noise

Apart from Fox and Lu's channel-based matrix method, different approaches have also been suggested to directly add effective noise to the channel open fraction to preserve the structure of the HH equation. As a result, different forms of colored noise have been proposed to be added to channel conductances in these effective LAs. Here, we discuss two representative approaches of this class introduced by Linaro *et al* and Güler [79, 82]. Again, in principle the open probability should be confined by 0 and 1. However, in order to achieve an adequate numerical approximation to the interspike interval statistics of the Markov method, the open fractions were set free to evolve without boundary conditions. As a result, the simulations of these two models would break down at small channel number. It was claimed by Linaro *et al* that their model is valid under the condition that the channel number is large. Therefore, with respect to these two effective approaches, we will not discuss the case of small channel number, such as $N < 500$.

4.4.1. Linaro et al approach (Linaro LA)

In this model, colored noises are added to the channel open fraction [79]; see also [58]. The noise is derived as an approximation of the fluctuations in the open channel count for a fixed number of subunits in the gating states n, h, and m. These gating variables describe the fraction of open subunits in the membrane patch, while the changes in membrane potential are determined by the open channel number. For infinite channel number, of course, the products m^3h and n^4 determine correctly the open fractions, but at finite channel numbers binomial distributions govern the open counts at fixed voltage. These distributions

can then be approximated by Gaussian distributions. In [79], the noise is given by the sum of a set of independent Ornstein–Uhlenbeck (OU) processes, which describe colored Gaussian noise:

$$\rho_{\mathrm{Na}} = m^3h + \sum_{i=1}^{7}\chi_i, \tag{51}$$

$$\rho_{\mathrm{K}} = n^4 + \sum_{i=1}^{4}\zeta_i. \tag{52}$$

The deterministic gating variables $w = \{m, h, n\}$ still obey equation (5). The 11 new stochastic variables χ_i and ζ_i are written as follows [79]:

$$\tau_{\mathrm{Na},i}\frac{\mathrm{d}\chi_i(t)}{\mathrm{d}t} = -\chi_i(t) + \sigma_{\mathrm{Na},i}\sqrt{2\tau_{\mathrm{Na},i}}\xi_{\mathrm{Na},i}(t), \tag{53}$$

$$\tau_{\mathrm{K},i}\frac{\mathrm{d}\zeta_i(t)}{\mathrm{d}t} = -\zeta_i(t) + \sigma_{\mathrm{K},i}\sqrt{2\tau_{\mathrm{K},i}}\xi_{\mathrm{K},i}(t), \tag{54}$$

where $\sigma_{\mathrm{Na},i}$, $\sigma_{\mathrm{K},i}$, $\tau_{\mathrm{Na},i}$, $\tau_{\mathrm{K},i}$ are voltage-dependent expressions, which can be found in [79]. $\xi_{\mathrm{Na},i}(t)$ and $\xi_{\mathrm{K},i}(t)$ are also Gaussian white noises with zero means and unitary variances.

4.4.2. Güler approach (Güler LA)

This model, like the Linaro *et al* approach, intends to preserve the original structure of the HH equations and to take into account the fluctuations related to channel states. Noise is added to both the gating fractions and the conductance. The model distinguishes the uncertainty in the number of gating fractions from what is here called the gate-to-channel uncertainty. The latter refers to the different configurations in which a given number of, say, *n*-gates can be distributed to the channels resulting in a variability of the open channel number. To take the gate-to-channel uncertainty into account, the author introduces equations of motion of Brownian harmonic oscillators to formulate colored noise terms [82]. The full set of equations for the noises is then

$$\rho_{\mathrm{Na}} = m^3h + \sqrt{\frac{m^3\left(1-m^3\right)}{N_{\mathrm{Na}}}}q_{\mathrm{Na}}, \tag{55}$$

$$\rho_{\mathrm{K}} = n^4 + \sqrt{\frac{n^4\left(1-n^4\right)}{N_{\mathrm{K}}}}q_{\mathrm{K}}, \tag{56}$$

$$\tau_{\mathrm{Na}}\frac{\mathrm{d}q_{\mathrm{Na}}}{\mathrm{d}t} = p_{\mathrm{Na}}, \tag{57}$$

$$\tau_{\mathrm{K}}\frac{\mathrm{d}q_{\mathrm{K}}}{\mathrm{d}t} = p_{\mathrm{K}}, \tag{58}$$

$$\tau_{\mathrm{Na}}\frac{\mathrm{d}p_{\mathrm{Na}}}{\mathrm{d}t} = -\gamma_{\mathrm{Na}}p_{\mathrm{Na}} - \upsilon_{\mathrm{Na}}^2\delta_{\mathrm{Na}}q_{\mathrm{Na}} + \gamma_{\mathrm{Na}}T_{\mathrm{Na}}\delta_{\mathrm{Na}}\xi_{\mathrm{Na}}, \tag{59}$$

$$\tau_{\mathrm{K}}\frac{\mathrm{d}p_{\mathrm{K}}}{\mathrm{d}t} = -\gamma_{\mathrm{K}}p_{\mathrm{K}} - \upsilon_{\mathrm{K}}^2\delta_{\mathrm{K}}q_{\mathrm{K}} + \gamma_{\mathrm{K}}T_{\mathrm{K}}\delta_{\mathrm{K}}\xi_{\mathrm{K}}, \tag{60}$$

where the parameters τ_{Na} and τ_{K} correspond to the unit time of 0.01 ms. The $\delta_{\mathrm{Na}} = \alpha_m(1-m) + \beta_m m$ or $\delta_{\mathrm{K}} = \alpha_n(1-n) + \beta_n n$ describe how fast a channel state loses memory at a microscopic timescale. The constants γ_{Na}, γ_{K}, υ_{Na}, υ_{K}, T_{Na}, and T_{K} and the variables q_{Na}, p_{Na}, q_{K}, and p_{K} are all nondimensional. The values of these constants can be found in [82]. The ξ_{Na} and ξ_{Kx} are Gaussian white noises with zero means and unitary variances. Gate variables *m*, *n*, and *h* have the same expressions as in the identical subunit-based LA.

4.5. Comparison of different LAs

In order to discuss the performance of Langevin approaches, different action potential statistics have been investigated and compared with the Markovian HH model. These statistical parameters include the steady state statistical properties (i.e. mean, standard deviation, autocorrelation) of the fraction of open channels under voltage clamp [58, 60, 61, 78, 79], the statistic behaviors responding to stimulus current pulse (i.e. firing efficiency, mean and standard deviation of spike latency, and jitter) [55, 79], the statistic action potentials responding to DC current (i.e. mean and standard deviation of action potential, the interspike interval, spike amplitude and spike width) [60, 62, 78, 79, 81], the power spectral densities of membrane voltage [79], the information rates of spiking and nonspiking membranes [57], and the bifurcation diagram of the membrane voltage against DC current [62].

By comparing different statistical variables, different evaluations on the performance of LAs are derived. In this review, we will mainly focus on the comparison of the action potential statistics responding to DC current, including the mean and standard deviation of action potential, the interspike interval, and spike amplitude.

The number of K^+ channel ranges from 500 to 5000 in most calculations in the paper. The running length was 250 s for the simulations of Langevin approaches and extended to 500 s for the Markov method when the number of K^+ channel is larger than 3000. When the increasing voltage passes a threshold like -60 mV and the reached peak before going back to the threshold is at least 30 mV higher than the threshold, the action potential is recorded. In this way, the aborted spikes with small amplitude can be discarded. The implementation of the Markovian method follows the protocol as described in II. C of [62].

4.5.1. Subunit-based LAs with rescaled noise

The subunit-based Langevin approaches are obtained by approximating the Markov model through adding Gaussian noise terms to the differential equations of subunits [15, 20]. Thus, although the Langevin approaches will be invalid at small channel number, one may expect that the Langevin approaches would converge to the Markov model as the channel number increases. However, in comparison to the Markov model, Sengupta *et al* showed that the identical subunit approach underestimates the channel noise, resulting in an overestimation of information rates

with channel number at 6000 Na^+ and 1800 K^+ channels [57]. This result indicates that the Langevin model may not be suitable for accurately simulating channel noise in neurons, even in simulations with large numbers of ion channels [57]. The same conclusion has also been drawn with other biological systems, including the intracellular calcium signals [39, 40, 78] and pancreatic β cells [42].

As shown in figure 3, both the identical and independent subunit LAs underestimate the noise intensity. As a result, in order to better approximate the Markovian channel noise, Huang *et al* considered a set of scaling parameters with $\lambda_w \geqslant 1$ ($w = n, m, h$) to enlarge the noise intensity for subunit-based LAs [77].

There are three different types of subunit in the HH model, thus a set of optimal factors λ_n, λ_m, and λ_h were determined by comparing the error of the action potential statistics between the standard stochastic HH model and the subunit LAs. Numerical simulations indicate that a varying of λ_h in the range of 1.0 to 3.0 has a negligible effect on stochastic activities by identical subunit LA. This may be related to the fact that the h-gate is a slow inactivation variable of Na^+ channels. As illustrated in figure 3, the identical subunit LA rescaled by two optimized factors $\lambda_n = 2.0$ and $\lambda_m = 1.8$ provides satisfied mean voltage and mean interspike intervals when compared with the standard values [77]. The simulation results implied that one could alternatively use such an adhoc approach to find a set of parameters of λ_h, λ_m and λ_n for the rescaled LA to nicely match the interspike interval given by the Markov HH method.

With respect to the independent subunit LA, simulation shows that a varying of λ_h or λ_m has a negligible effect on the quantities of interest. Then $\lambda_h = \lambda_m = 1$ is considered only as λ_n is adjusted. Simulation results are given in figure 3 with $\lambda_n = 3$ [77]. It is evident that the computed quantities are improved significantly and are comparable with those obtained by the rescaled identical subunit LA. Here we conclude that the independent subunit-based LA benefits more from such a rescaling scheme than does the identical method.

4.5.2. The limitation of subunit-based LAs

The assumption of subunit-based LAs has long been challenged and has been demonstrated to be intrinsically inaccurate, because the subunit-based noise fundamentally differs from that of the Markovian chain model [58]. Although a simple LA can yield good results for a large number of some ion channels such as calcium signaling models [87], the accuracy is actually model-dependent. For example, the identical subunit LA provides stronger noise for the Li–Rinzel model [78], but weaker noise for the HH model [17, 58]. Even though the accuracy can be improved with the rescaled-noise scheme for the HH model as implemented here and for the Li–Rinzel model first performed in [78], it is an adhoc approach that calls for preliminary simulations to determine the scaling factors.

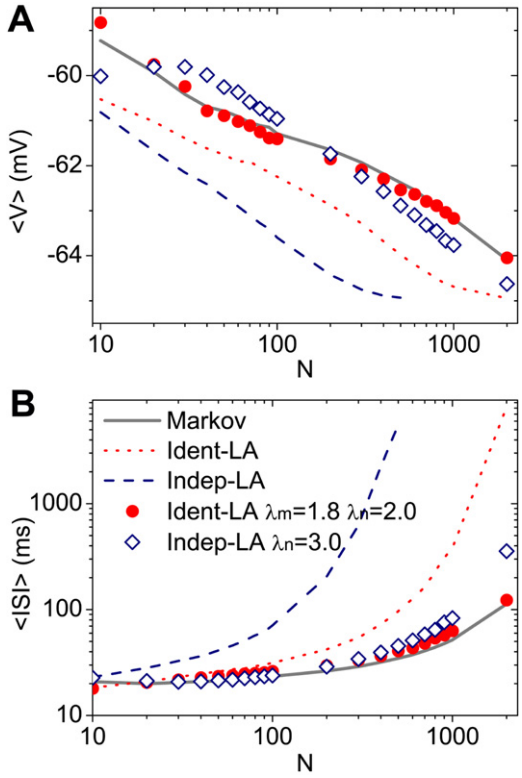

Figure 3. The comparison of the mean membrane potential (a) and the mean interspike interval (b) of the stochastic HH model as a function of channel number N from 10 to 2000 among Markov method (solid line), Fox–Lu identical subunit-LA (dot line), Fox–Lu independent subunit-LA (dashed line), rescaled identical subunit-LA at $\lambda_n = 2.0$, $\lambda_m = 1.8$, and $\lambda_h = 1.0$ (solid circle) and rescaled independent subunit-LA at $\lambda_n = 3.0$, $\lambda_m = 1.0$, and $\lambda_h = 1.0$ (open square).

Bruce has proposed that a source of the inaccuracy is that the Fox–Lu subunit LA does not adequately describe the combined behavior of the multiple activation of subunits in each Na^+ and K^+ channel [56]. Bruce suggested that the stochastic term added in the dynamics of subunit fractions should be correlated and have a non-Gaussian noise with a non-zero mean, rather than an uncorrelated, zero mean Gaussian noise.

By analyzing three LA models, i.e. the identical subunit-based LA, the independent subunit-based LA and the channel-based LA, Goldwyn *et al* showed that the channel-based approach can capture the statistical behaviors of the Markov HH model better than the two subunit LAs [58]. This comparison indicates that the temporal correlation in the channel noise is determined by the combinatorics of bundling subunits into channels, but the subunit-based approaches do not correctly account for this structure.

4.5.3. Statistics of action potentials by channel-based LAs

Now that subunit-based Langevin approaches fail to converge to Markov dynamics even at large channel

number [55, 56, 76], a timely question is to what extent the channel-based LAs approximate the Markov chain simulation. Unlike the subunit-based models, channel-based models consider the intrinsically cooperative action of multiple gates that constitute a single channel. However, the current difficulty is how to properly carry out Fox and Lu's channel-based model or how to impose channel noise to govern the conduction with different methods. This issue has been partially discussed among the channel-based matrix methods in [62, 81, 84]. In the current review, we discuss if the statistical results obtained by these LAs converge to those given by the Markovian method. The discretized LA is not considered here because it would not help improve the accuracy when N is bigger than 500.

As shown in figure 4, the mean voltage, spike amplitude and spike width derived by these LAs converge to the results by the Markovian method. However, some of them fail in higher order statistics, including the skewness (equation (61)) and kurtosis (equation (62)) of action potentials, which are defined as

$$\text{Skewness} = \frac{\sum_{i=1}^{M}\left(V_i - \langle V\rangle\right)^3}{(M-1)\delta^3} \tag{61}$$

$$\text{Kurtosis} = \frac{\sum_{i=1}^{M}\left(V_i - \langle V\rangle\right)^4}{(M-1)\delta^4} - 3 \tag{62}$$

where M is the number of data points, V_i is the voltage, $\langle V\rangle$ and δ are the mean and standard deviation of V_i respectively. As shown in figure 5, except for the Orio LA, the values of skewness and kurtosis obtained by those unbounded approaches, i.e. the original Fox–Lu LA, Linaro LA and Güler LA, deviate from the results given by the Markov method. However, the two bounded approaches, i.e. the reflected approach and truncated-restored approach, can replicate the two values given by the Markov method.

The most important parameter is the spiking frequency, or the interspike interval (ISI), because it is believed to be used to encode neuronal information. Besides the mean ISI, we also discuss the ISI distribution in detail. Figure 6 shows the difference of the mean ISI obtained by the Markov method and the Langevin approaches against the channel number. The comparison in figure 6 clearly reveals the shortcoming of some Langevin approaches. Among these LAs, the truncated-restored approach as well as the unbounded Orio's approach remains accurate as the channel number increases. Previously, it was demonstrated in [62] that the restoring process is essential because when the reflection is followed by the restoring operation, it can achieve convergence as well. The reflected LA gives a longer ISI. This is because the strong noise has been cut off during the reflected procedure and smaller noise intensity produces longer ISIs. As to the unbounded Orio approach, mainly due to the absolute values applied in the square root arguments, the noise

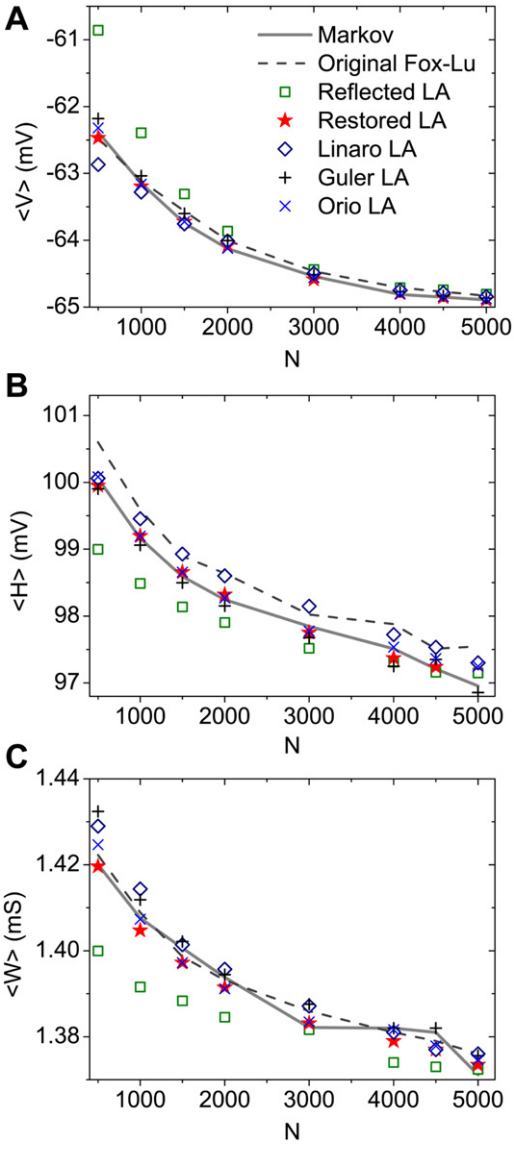

Figure 4. The comparison of mean membrane voltage (a), spike amplitude (b) and width (c) as a function of channel number N from 500 to 5000 for Markov method (solid line), unbound Fox–Lu channel-based LA (dashed line), reflected LA (green square), truncated and restored LA (red star), Linaro LA (blue lozenge), Güler LA (black plus) and Orio LA (blue cross). Here the stimulus current $I_{\text{stim}} = 0$.

intensity is not affected as well. On the other hand, the original LA and the two effective methods (Güler LA and Linaro LA) generate shorter ISI than with the Markov method, indicating that the noise intensities considered in these three LAs are larger than the Markovian noise.

The ISI distributions at the channel number of 1000 and 5000 with the stimulus current $I_{\text{stim}} = 0$ are discussed in figure 7. At small channel number with $N = 1000$, the ISI is mainly distributed in the range of smaller than 300 ms because of the large channel noises. Figure 7(a) shows that all these different LAs can nicely reproduce the ISI distribution given by the Markov method. However, at $N = 5000$, the reflected LA, truncated and restored LA, Güler LA and Orio LA

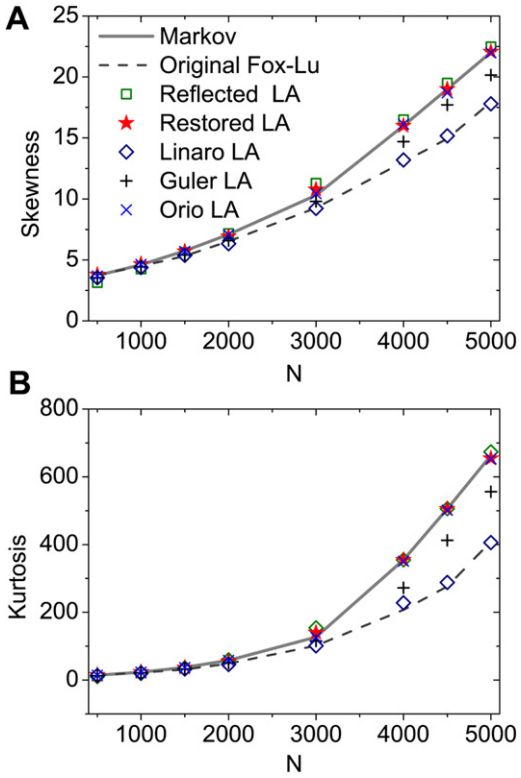

Figure 5. The comparison of mean skewness (a) and kurtosis (b) of voltage as a function of channel number N from 900 to 5000 among Markov method (solid line), unbound Fox–Lu channel-based LA (dashed line), reflected LA (green square), truncated and restored LA (red star), Linaro LA (blue lozenge), Güler LA (black plus) and Orio LA (blue cross). Here the stimulus current $I_{\text{stim}} = 0$.

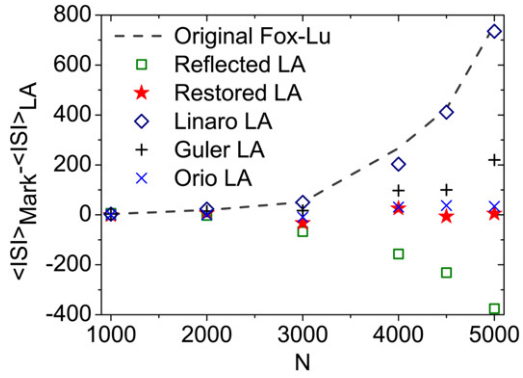

Figure 6. Error of mean interspike interval with respect to Markov method as a function of channel number N from 1000 to 5000. The mean ISI at $N = 1000$ by Markov method is about 51.6 ms. The comparison is among the original Fox–Lu's unbound channel-based LA (dash line), reflected LA (green square), truncated and restored LA (red star), Linaro LA (blue lozenge), Güler LA (black plus) and Orio LA (blue cross). Here the stimulus current $I_{\text{stim}} = 0$ μA.

give better ISI distribution than the original Fox–Lu LA and Linaro LA. The ISI distributions derived from the original Fox–Lu LA and Linaro LA are over-concentrated in the region of small ISI.

Recently, Rowat and Greenwood calculated distributions of ISI of the neuron model responding to a certain stimulus at $I_{\text{stim}} = 6$ μA cm^{-2} and found generally similar ISI histograms for the Markovian method, the original Fox–Lu LA, as well as the Linaro *et al* Güler and Orio approaches. The Güler approach was deemed computationally faster than the other methods although the ISI distributions are not as close to the Markovian method as for the original Fox–Lu LA [83]. At $I_{\text{stim}} = 6$ μA cm^{-2}, the deterministic HH neuron is right below the bifurcation point (approximately $I_{\text{stim}} = 6.5$ μA cm^{-2}) to generate the periodic spikes. Thus, for the stochastic HH model with $I_{\text{stim}} = 6$ μA cm^{-2}, the channel noise can easily trigger action potentials. In this review, the ISI distributions at the channel number of 1000 and 10000 with the stimulus current $I_{\text{stim}} = 6$ μA cm^{-2} are also discussed. As shown in figure 8, The ISI distributions by these channel-based Langevin approaches agree well with that derived from the Markov method, except for the Güler LA which gives a little lower probability of big ISI at $N = 1000$.

The Langevin methods and their performance are summarized in table 1. This comparison indicates that, if only the noise intensity is properly maintained, either the bounded approach, like the truncated and restored approach, or the unbounded approach, like the Orio's approach, is able to replicate the discussed parameters from the Markov method.

4.5.4. Key role of bounded and discrete open fractions in resting state

In order to discuss the origin of these different performances among different LAs, we analyze the properties of the zero open fraction by the reflected LA and truncated-restored LA, and the non-positive channel open fraction by the original Fox–Lu LA, Linaro LA, Güler LA and Orio LA. Figure 9 plots the results of the probability of all channels in closed states (panels A and B for K^+ and Na^+ channels, respectively) and the mean time of staying in the closed state for all channels (panels C and D) against N. Deterministically, without any stimulus, the HH neuron model shows an open fraction of 0.01 for the K^+ channels and 0.00017 for the Na^+ channels, respectively. As a result at $N = 1000$ there are on average 10 open K^+ channels, and the Markov method shows that the probability of all K^+ channels in closed state exponentially decays to 10^{-5}. However, at $N = 5000$ there are on average 2.6 open Na^+ channels, and the Markov method indicates that the probability of all Na^+ channels in closed state is still as large as 0.3. Figures 9(c) and (d) show that the corresponding mean time of staying in closed state obtained with the Markov method decreases rapidly down to the computation time step (0.01 ms) at $N > 1000$ for K^+ channels, but only down to 0.1 ms for Na^+ channels.

From figures 9(a) and (b), one can see that only the discretized LA can reproduce the probability of zero

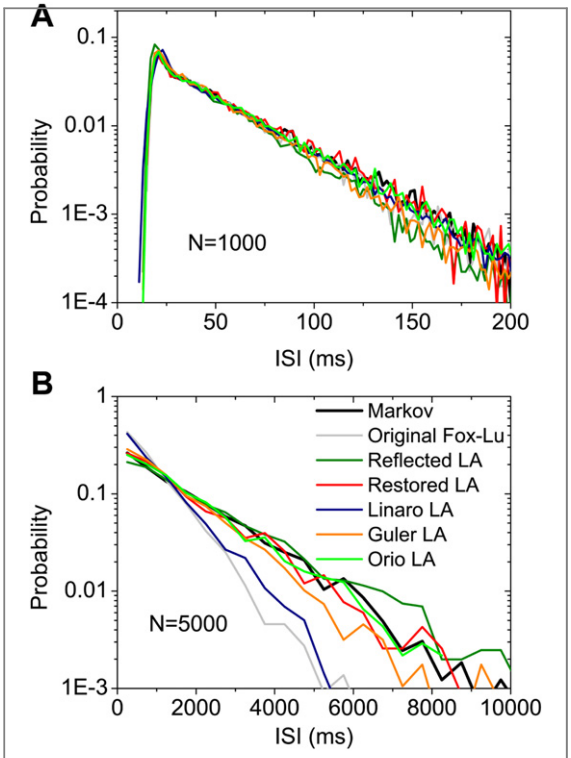

Figure 7. ISI distributions with the channel number of (a) 1000 and (b) 5000. The comparison is among Markov method (black), original Fox–Lu channel-based LA (gray), reflected LA (olive), truncated and restored LA (red), Linaro LA (blue), Güler LA (orange) and Orio LA (green). Here the stimulus current $I_{stim} = 0$.

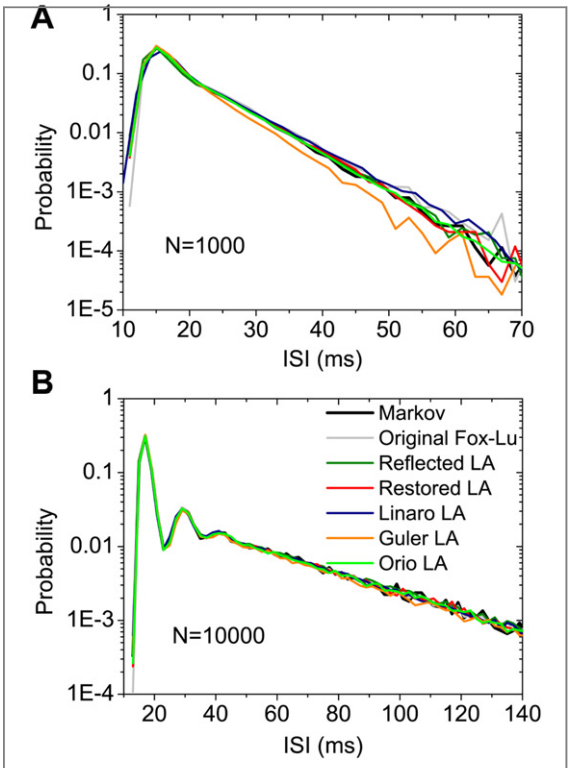

Figure 8. ISI distributions at (a) N = 1000 and (b) 10000 in the presence of constant current $I_{stim} = 6\ \mu A\ cm^{-2}$. The comparison is among Markov method (black), original Fox–Lu channel-based LA (gray), reflected LA (olive), truncated and restored LA (red), Linaro LA (blue), Güler LA (orange) and Orio LA (green).

channel open fraction for both K^+ and Na^+ channels. The truncated-restored LA gives a correct probability of zero channel open fraction for K^+, but a slightly smaller probability of zero open fraction for Na^+ channels. In fact, compared to the Markov method, the original Fox–Lu LA, Linaro LA and Güler LA typically give a large probability of negative channel open fraction for K^+ channels and a small negative channel open fraction for Na^+ channels. In particular the Orio LA is as good as the truncated and restored approach for K^+ channels (figures 9(a) and (b)), however, it resembles the original Fox–Lu LA for Na^+ channels (figures 9(c) and (d)). Noting that with a negative K^+ (or Na^+) open fraction, the K^+ (or Na^+) current will change its flux direction. As a result, these negative open fractions yield a larger inward Na^+ current and a less outward K^+ current than the Markov method, determining a more excitable system with shorter ISI.

As shown in figure 9(d), all LAs can give a constant mean time in closed state for Na^+ channels at large N. However, figure 9(c) reveals that all the LAs are not able to provide a satisfying approximation for the mean time of staying in the closed states of all K^+ channels. This discussion indicates that there may be an intrinsic shortcoming of master-equation LAs which fails to reproduce the behavior of all channels staying in closed state. An accurate Langevin approach to represent the Markov channel dynamics is still lacking.

4.5.5. Significance of time-dependent diffusion matrix

One advantage of the bounded approach is that the diffusion matrices are time dependent. As we know, the mean values of the open fractions only depend on the voltage, whereas the variances of the open fractions reduce as the channel number increases. Thus, variances are overlooked when the mean values of the fractions are used in the diffusion matrix. As a consequence, steady-state approximation would lead to underestimated noise at small channel number and overestimated noise when the number of the channel is large.

Two hybrid approaches are proposed here to demonstrate the limitation of quasi-stationary assumption of the diffusion matrices in the unbounded original Fox–Lu LA especially at big channel number. In hybrid 1, the diffusion matrices in the original Fox–Lu LA are calculated with the truncated-restored LA. As a result, the diffusion matrices vary with time. In hybrid 2, the diffusion matrices in truncated-restored LA are estimated based on the equilibrium fractions as in the original Fox–Lu LA. As illustrated in figure 10, the mean ISI provided by hybrid 1 agrees with that by the Markov method, whereas hybrid 2 underestimates the mean ISI as the original Fox–Lu LA does, indicating that the dependence of the diffusion matrices upon time is of importance at big channel number. As illustrated in figures 4 to 8, the results given by Linaro LA are close to those

Table 1. Comparison of different channel-based LAs.

Method	References	Master Equation	[0,1][a]	Noise type	Converged mean values at large N
Original Fox–Lu LA	[15, 58]	Yes	No	White Gaussian	V^c,H^d,W^e
Reflected LA	[61]	Yes	Yes	White Gaussian	V,H,W, S^f, K^g
Restored LA	[62]	Yes	Yes	Colored Gaussian[b]	V, H, W, S, K, ISI
Linaro LA	[79]	No	No	Colored Gaussian	V, H, W
Güler LA	[82]	No	No	Colored Gaussian	V, H, W
Orio LA	[60]	Yes	No	White Gaussian	V, H, W, S, K, ISI

[a] Boundary condition.
[b] The added noise is white Gaussian, but after truncated and restored processes, it becomes colored Gaussian.
[c] Membrane voltage.
[d] Spike amplitude. The difference between the peak of a spike and the threshold of −60 mv.
[e] Spike width.
[f] Skew of membrane voltage.
[g] Kurtosis of membrane voltage.

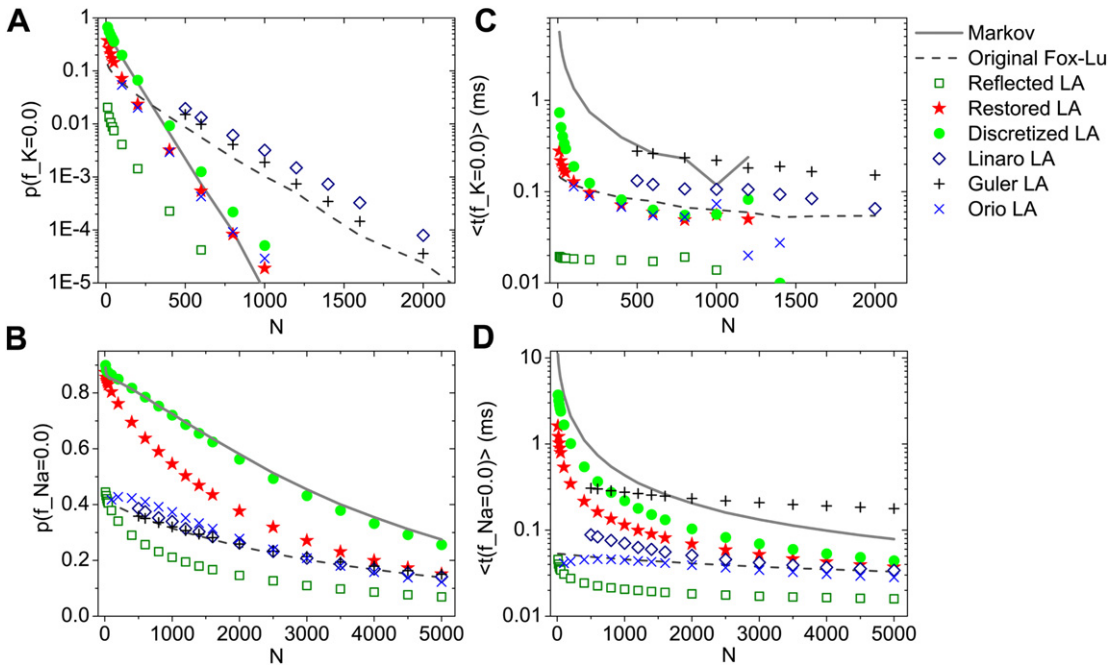

Figure 9. The comparison of the closing probability of K^+ channel (a) and Na^+ channel (b) respectively and the mean time staying in closed state for K^+ channel (c) and Na^+ channel (d) respectively. The comparison is among Markov method (solid line), original Fox–Lu channel-based LA (dashed line), reflected LA (green square), truncated and restored LA (red star), discretized LA (brown circle), Linaro LA (blue lozenge), Güler LA (black plus) and Orio LA (blue cross). Here the stimulus current $I_{stim} = 0$ μA.

given by the original Fox–Lu LA, which agrees well with the conclusion drawn in [60, 84]. Both methods involve a steady-state approximation in the stochastic terms, which accounts for the identical inaccuracies.

4.5.6. Indispensable restoration process

Here we demonstrate that the restoration process proposed in the truncated-restored LA is an indispensable complement to the Langevin approaches with standard diffusion matrix. Huang *et al* have provided the evidence that the performance of the reflected LA becomes as good as the truncated-restored LA once the restoration process is added [62]. We call the reflected LA plus post-processing reflected LA+R. Likewise, in this review we applied the truncation and restoration to the unbounded fractions of channel states in Orio LA (Orio LA+TR). As illustrated in figures 11(a) and (b), the statistics of action potential of the Orio LA, such as mean voltage and the ISI, are not influenced at all by the post-processing, while the closing probability ($p(f\_Na = 0.0)$) and the mean time of staying in closed state ($\langle t(f\_Na = 0.0)\rangle$) become much better, as shown in figures 11(c) and (d). Therefore the restoration process may be a general step for the matrix-based Langevin approaches.

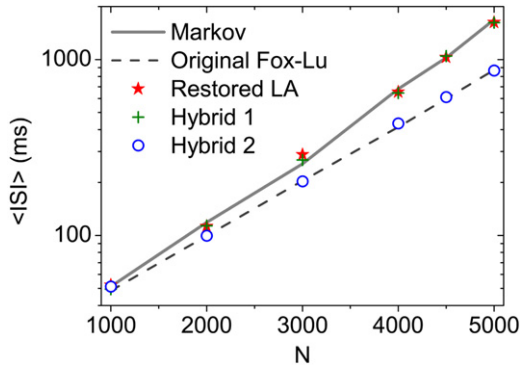

Figure 10. Mean interspike interval as a function of channel number N from 1000 to 5000. The comparison is among the Markov method (solid line), original Fox–Lu's unbound channel-based LA (dash line), truncated and restored LA (red star), hybrid 1 (plus) and 2 (circle). In hybrid 1, the diffusion matrix in the original Fox–Lu's unbound LA is calculated with the truncated and restored approach. In hybrid 2, the diffusion matrix in truncated and restored LA is approximated by using equilibrium fractions. Here the stimulus current $I_{\text{stim}} = 0$.

4.5.7. Computational efficiency

Another important issue is the relative computational efficiency of various Langevin approaches. As pointed out by Pezo *et al* in [84], Güler LA is the fastest among the channel-based LAs listed above. However, they did not use a unit programming language. In this review we show a more precise comparison of the computational efficiency by using a single programming language C. With respect to the running length of 160 s and the time step of 0.01 ms, the computational time of the original Fox–Lu LA is 263.52 s which is taken as the reference. Here we focus on one single channel number $N = 1000$. The computational time given by different approaches are listed in table 2. As presented in table 2, the original Fox–Lu LA as well as the truncated and restored LA is about one magnitude slower than the others due to the demanding calculation of the root square of the diffusion matrix. The time of the subunit-based LAs is about half of that by the fastest channel-based LA, namely Güler LA. In fact, the simple formulation of the square-root diffusion matrices derived for the Orio LA is identical to that introduced by the reflected LA. Therefore, in terms of numerical effort, they provide nearly the same computational efficiency. In addition, it should be stressed that the reflected LA and the Orio LA with post-processing (reflected LA+R and Orio LA+TR) exhibit the same computational efficiencies with the reflected LA and Orio LA respectively, indicating the negligible computational cost of the post-processing.

5. Conclusions and outlook

Since 1994, when Fox and Lu proposed the Langevin approaches to simulate the stochastic HH neuronal model [15, 20], these approaches have been widely applied for the study of noisy channel dynamics. However, none of these approaches guarantees a precise description of channel noise in the neuronal system. In consequence, the use of the over-simplified noise approximations in stochastic differential equations may thereby lead to qualitatively correct but quantitatively incorrect conclusions. Only recently, several groups have become interested in how to construct an improved Langevin approach in order to better describe the Markovian channel dynamics. In this paper we reviewed the newer developments of Langevin approaches to the intrinsic Markovian noise in the standard stochastic HH model.

In order to simulate the Markovian channel dynamics, the original Langevin approach proposed by Fox and Lu naturally assumed an uncorrelated, zero-mean Gaussian noise [15, 20]. However, the simulations by the truncated and restored LA indicated that the simple Gaussian noise cannot adequately describe the Markovian channel dynamics, and the inaccuracy has shown up even at large channel numbers [62]. Thus, an important question is how to construct a correct noise term in the Langevin approach and where to add the noise to the equations in order to correctly describe the Markovian channel dynamics [80].

The first issue discussed is the distinction of subunit-based and channel-based models. Because channel noises depend on the combinatorics of subunits of a channel, the channel-based LA can describe the channel noise better than the subunit-based LA. The simulation results indicate that the diffusion matrix technique using the time-dependent channel-state fractions will compare better to the Markov method than using the equilibrium channel-state fractions. In a different line of research, noise terms were derived that can be added to the original HH differential equations [79, 80, 82]. These effective approaches are not limited to explicit Markov chains because their empirical parameters can be estimated from the conduction fluctuation measured in experiment [80]. The models also implicate time-correlated colored noise in stimulating the Markovian processes of channel transitions [62, 79, 82]. However, we presented evidence that the discussed two effective LAs are not as good as the bounded Fox and Lu LA with the truncated and restored fractions or the unbounded Orio LA. Under constant current, the original Fox–Lu LA was proved to provide a better distribution of interspike interval than was provided by the two effective approaches [83]. A better effective approach is still lacking.

Among these Langevin approaches, the bounded truncated-restored LA and the unbounded Orio LA are equally good, and provide the best approximations to the exact microscopic simulation. However, the Orio LA lacks the biologically meaningful boundary of the channel-state fractions. In fact, most of the improved Langevin approaches simply allow the un-

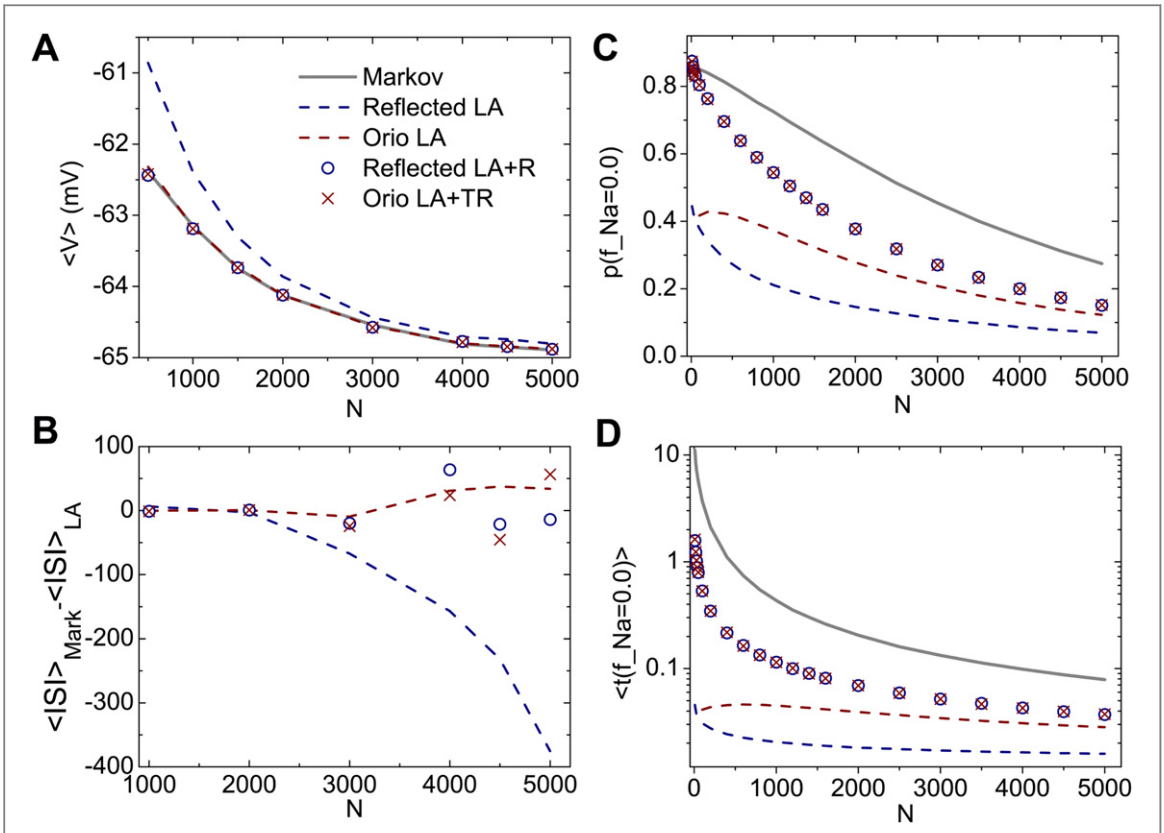

Figure 11. The mean voltage (a), error of mean interspike interval (b), closing probability of Na^+ channel (c) and the mean time staying in closed state of Na^+ channel (d). The comparison is among Markov method (solid line), reflected LA (dashed blue line), Orio LA (dashed red line), reflected LA plus restoration (+R) (blue circle) and Orio LA plus truncation and restoration (+TR) (red cross). Here the stimulus current $I_{stim} = 0$.

Table 2. Computational efficiency of different LAs.

Method	References	Relative comput. efficiency
Ident. LA	[15, 20],	0.078
Indep. LA	[40]	0.12
Original Fox–Lu LA	[15], [58]	1.0
Restored LA	[62]	1.0
Reflected LA	[61]	0.23
Reflected LA+R	[62]	0.23
Linaro LA	[79]	0.28
Güler LA	[82]	0.15
Orio LA	[60]	0.23
Orio LA+TR		0.23

Note. The running length is 160 s and the time step is 0.01 ms. The recorded time of the original Fox–Lu LA is 263.52 s. The relative computational efficiency is the ratio of the recorded time to 263.52 s.

physical open fractions driven by the noise [58, 60, 79, 82]. In this review, we show that this problem can be well solved with the truncated and restored procedure proposed by Huang *et al* (figures 4–11), implying that the restoration of the residual fractions after the truncation procedure may be indispensable and applicable to other stochastic channel models. Among all the reviewed LAs, taking the computational efficiency into account, the combination of the Orio LA or the reflected LA with the truncated-restored LA, such as Reflected LA+R or Orio LA+TR, provides the most accurate and simultaneously physically meaningful approximation to the Markovian dynamics.

Langevin equations are constructed from the master equations which are the heart of simulations of biochemically reactions and ion-channel dynamics if the number of molecules is small. Normally, the Langevin approaches, especially the effective approaches, cannot accurately replicate the properties of the Markov model at small channel number, such as a few tens of channels in the patch. However, there are some biological situations where only a few tens of channels are observed in clusters, such as channels in the dendritic spine or in an axon node. Other examples are the Ca^{2+} releasing IP_3R channels and RyR channels which are spatially organized in clusters with only a few or several tens of IP_3R and ryanodine receptors in the ER and SR membranes [50, 51, 88–90]. Thus, these systems call for the effective Langevin approaches especially for capturing the Markov channel dynamics at a small membrane patch area. The first effort proposed in [81] indicates that the continuous-to-discrete treatment is necessary in order to catch the intrinsically discrete property of channel state fractions at small membrane patch areas (see also [91]). Actually, the discretization procedure is feasible only when the boundary condition is satisfied, thus it is important to

use a bounded method. The discretization as well as the restoration as mentioned above are helpful to the methodological advances of numerical algorithms. Their relevance to the impact on excitability of neural systems is not clear yet. However, the encouraging results throw light on future improvement.

In fact, we still lack a universal and consistent Langevin approach to accurately represent the Markov channel dynamics. A Markov chain can be completely described by master equations. Different approximate approaches have been developed to solve the master equations in a variety of biochemical networks [92, 93]. A generating function approach has been proposed for the Markovian process by mapping the master equation into a wave equation, and has been applied to a variety of signal transduction problems [94, 95]. A Brownian-ratchet-like stochastic theory has recently been developed for the electrochemical membrane system of the HH model [96]. We believe that the development of these stochastic theories may shed light on how to improve the Langevin approach.

Besides the discussion of the effects of channel noise, a more fundamental question is how to characterize the channel noise accurately. During the last thirty years, fractal ion-channel behavior and history-dependent ionic current signals have been captured in experiments through analyzing the patch-clamp data [97–102]. Moreover, the analysis of the power spectra of nanochannel currents showed that such currents have the properties of the so-called $1/f$ (flicker) noise [103–105]. Actually a biologically realistic neuronal system is complex with composite axon and dendritic structures, showing a non-Markovian channel dynamics.

The channel noise discussed in the paper is a specific example of the widespread phenomenon of noise in complex biological systems. Stochasticity has been shown to widely exist in subcellular systems, including those involved in synaptic transmission, cellular signaling networks and regulation of gene expression, because these systems include a relatively limited number of constituent molecules that interact nonlinearly [106–110]. The accurate simulation of stochastic chemical reaction with Langevin approaches is an active area of research.

The results reviewed in this paper concern the recently developed Langevin approaches on stochastic channel dynamics, aiming to accurately represent Markovian channel noise. Given the increasing interest in biological stochastic processes, the accurate simulation of the channel noise by the Langevin model becomes an important issue for the studies of stochasticity in molecular systems. The accurate Langevin approaches may reveal how channel behavior affects spike timing, reliability, propagation, and other aspects of neural dynamics. These Langevin approaches could be principally applicable in other stochastic systems. With the accurate Langevin approaches, more quantitative insights on how biological noise modulates electrophysiological dynamics and function in cellular systems can emerge.

Acknowledgments

Shuai acknowledges support from the China National Funds for Distinguished Young Scholars under grant 11125419, the National Natural Science Foundation of China under grant 31370830, and the Fujian Province Funds for Leading Scientist in Universities. Rüdiger acknowledges support from the Deutsche Forschungsgemeinschaft (RU 1660 and IRTG 1740).

References

[1] Dayan P and Abbott L 2001 *Theoretical Neuroscience: Computational and Mathematical Modeling of Neural Systems* (Cambridge, MA: MIT Press)
[2] Hodgkin A L and Huxley A F 1952 A quantitative description of membrane current and its application to conduction and excitation in nerve *J. Physiol.* **117** 500–44
[3] Lecar H and Nossal R 1971a Theory of threshold fluctuations in nerves: I. Relationships mbetween electrical noise and fluctuations in axon firing *Biophys. J.* **11** 1048–67
[4] Lecar H and Nossal R 1971b Theory of threshold fluctuations in nerves: II. Analysis of various sources of membrane noise *Biophys. J.* **11** 1068–84
[5] Neher E and Sakmann B 1976 Single-channel currents recorded from membrane of denervated frog muscle fibres *Nature* **260** 779–802
[6] Neher E and Stevens C F 1977 Conductance fluctuations and ionic pores in membranes *Annu. Rev. Biophys. Bioeng.* **6** 345–81
[7] DeFelice L J 1977 Fluctuation analysis in neurobiology *Int. Rev. Neurobiol.* **20** 169–208
[8] Sigworth F J 1980 The variance of sodium current fluctuations at the node of Ranvier *J. Physiol.* **307** 97–129
[9] Schneidman E, Freedman B and Segev I 1998 Ion channel stochasticity may be critical in determining the reliability and precision of spike timing *Neural Comput.* **10** 1679–703
[10] Whitea J A, Rubinsteinb J T and Kay A R 2000 Channel noise in neurons *Trends Neurosci.* **23** 131–7
[11] Faisal A A, White J A and Laughlin S B 2005 Ion-channel noise places limits on the miniaturization of the brains wiring *Curr. Biol.* **15** 1143–9
[12] Faisal A A and Laughlin S B 2007 Stochastic simulations on the reliability of action potential propagation in thin axons *PLoS Comput. Biol.* **3** 1–13
[13] DeFelice L J and Isaac A F 1993 Chaotic states in a random world: Relationship between the nonlinear differential equations of excitability and the stochastic properties of ion channels *J. Stat. Phys.* **70** 339–54
[14] Strassberg A F and DeFelice L J 1993 Limitations of the Hodgkin–Huxley formalism: effects of single channel kinetics on transmembrane voltage dynamics *Neural Comput.* **5** 843–55
[15] Fox R F and Lu Y N 1994 Emergent collective behavior in large numbers of globally coupled independently stochastic ion channels *Phys. Rev.* E **49** 3421–31
[16] Chow C C and White J A 1996 Spontaneous action potentials due to channel fluctuations *Biophys. J.* **71** 3013–21
[17] Zeng S and Jung P 2004 Mechanism for neuronal spike generation by small and large ion channel clusters *Phys. Rev.* E **70** 011903

[18] Steinmetz P N, Manwani A and Koch C 2001 Variability and coding efficiency of noisy neural spike encoders *Biosystems* **62** 87–97

[19] Mainen Z F and Sejnowski T J 1995 Reliability of spike timing in neocortical neurons *Science* **268** 1503–6

[20] Fox R F 1997 Hodgkin–Huxley equations *Biophys. J.* **72** 2068–74

[21] Gammaitoni L, Hänggi P, Jung P and Marchesoni F 1998 Stochastic resonance *Rev. Mod. Phys.* **70** 223–88

[22] Jung P and Shuai J W 2001 Optimal sizes of ion channel clusters *Europhys. Lett.* **56** 29–35

[23] Adair R K 2003 Noise and stochastic resonance in voltage-gated ion channels *Proc. Natl Acad. Sci. USA* **100** 12099–104

[24] McDonnell M D and Abbott D 2009 What is stochastic resonance? definitions, misconceptions, debates, and its relevance to biology *PLoS Comput. Biol.* **5** e1000348

[25] Schmid G, Goychuk I and Hänggi P 2003 Channel noise and synchronization in excitable membranes *Physica* A **325** 165–75

[26] Yang L and Jia Y 2005 Effects of patch temperature on spontaneous action potential train due to channel fluctuations: coherence resonance *Biosystems* **81** 267–80

[27] Shuai J W and Jung P 2005 Entropically enhanced excitability in small systems *Phys. Rev. Lett.* **95** 1–4

[28] Shuai J W and Jung P 2006 The dynamics of small excitable ion channel clusters *Chaos* **16** 026104

[29] Dudman J T and Nolan M F 2009 Stochastically gating ion channels enable patterned spike firing through activity-dependent modulation of spike probability *PLoS Comput. Biol.* **5** e1000290

[30] Schmerl B A and McDonnell M D 2013 Channel-noise-induced stochastic facilitation in an auditory brainstem neuron model *Phys. Rev.* E **88** 052722

[31] Goychuk I and Hänggi P 2002 Ion channel gating: a first passage time analysis of the kramers type *Proc. Natl Acad. Sci. USA* **99** 3552–6

[32] Laughlin S B and Sejnowski T J 2003 Communication‡n neuronal networks *Science* **301** 1870–4

[33] Lindnera B, Garcia-Ojalvo J, Schimansky-Geier L and Neiman A 2004 Effects of noise in excitable systems *Phys. Rep.* **392** 321–424

[34] Destexhe A and Contreras D 2006 Neuronal computations with stochastic network states *Science* **314** 85–90

[35] Aldo Faisal A, Selen L P J and Wolpert D M 2008 Noise in the nervous system *Nat. Rev. Neurosci.* **9** 292–303

[36] Cannon1 R C, ODonnell C and Nolan M F 2010 Stochastic ion channel gating in dendritic neurons: morphology dependence and probabilistic synaptic activation of dendritic spikes *PLoS Comput. Biol.* **6** e1000886

[37] Schmid G, Li Y, Hänggi P and Schimansky-Geier L 2010 Spontaneous spiking in an autaptic Hodgkin–Huxley setup *Phys. Rev.* E **82** 061907

[38] Fisch K, Schwalger T, Lindner B, Herz A V M and Benda J 2012 Channel noise from both slow adaptation currents and fast currents is required to explain spike-response variability in a sensory neuron *J. Neurosci.* **32** 17332–44

[39] Shuai J W and Jung P 2002a Optimal intracellular calcium signaling *Phys. Rev. Lett.* **88** 068102

[40] Shuai J W and Jung P 2002b Stochastic properties of Ca^{2+} release of inositol 1,4,5-trisphosphate receptor clusters *Biophys. J.* **83** 87–97

[41] Shuai J W and Jung P 2003a Optimal ion channel clustering for intracellular calcium signaling *Proc. Natl Acad. Sci. USA* **100** 506–10

[42] Zhan X, Wu D, Yang L, Liu Q and Jia Y 2007 Effects of both glucose and IP_3 concentrations on action potentials in pancreatic β-cells *Eur. Biophys. J.* **36** 187–97

[43] Skupin A, Kettenmann H, Winkler U, Wartenberg M, Sauer H, Tovey S C, Taylor C W and Falcke M 2008 How does intracellular Ca^{2+} oscillate: by chance or by the clock? *Biophys. J.* **91** 2404–11

[44] Liao X L, Jung P and Shuai J W 2009 Global noise and oscillations in clustered excitable media *Phys. Rev. E* **79** 041923

[45] Skupin A, Kettenmann H and Falcke M 2010 Calcium signals driven by single channel noise *PLoS Comput. Biol.* **6** e1000870

[46] Rüdiger S, Shuai J W and Sokolov I M 2010 Law of mass action, detailed balance, and the modeling of calcium puffs *Phys. Rev. Lett.* **105** 048103

[47] Rüdiger S 2014 Excitability in a stochastic differential equation model for calcium puffs *Phys. Rev.* E **89** 062717

[48] Rüdiger S 2014a Stochastic models of intracellular calcium signals *Phys. Rep.* **534** 39–87

[49] Keizera J and Smith G D 1998 Spark-to-wave transition: saltatory transmission of calcium waves in cardiac myocytes *Biophys. Chem.* **72** 87–100

[50] Izu L T, Gil Wier W and William Balke C 2001 Evolution of cardiac calcium waves from stochastic calcium sparks *Biophys. J.* **80** 103–20

[51] Williams G S B, Huertas M A, Sobie E A, Saleet Jafri M and Smith G D 2007 A probability density approach to modeling local control of calcium-induced calcium release in cardiac myocytes *Biophys. J.* **92** 2311–28

[52] Gillespie D T 1976 A general method for numerically simulating the stochastic time evolution of coupled chemical reactions *J. Comp. Phys* **22** 403–34

[53] Gillespie D T 1977 Exact stochastic simulation of coupled chemical reactions *J. Phys. Chem.* **81** 2340–61

[54] Rüdiger S, Shuai J W, Huisinga W, Nagaiah C, Warnecke G, Parker I and Falckey M 2007 Hybrid stochastic and deterministic simulations of calcium blips *Biophys. J.* **93** 1847–57

[55] Bruce I 2007 Implementation issues in approximate methods for stochastic Hodgkin–Huxley models *Ann. Biomed. Eng.* **35** 315–8

[56] Bruce I 2009 Evaluation of stochastic differential equation approximation of ion channel gating models *Ann. Biomed. Eng.* **37** 824–38

[57] Sengupta B, Laughlin S B and Niven J E 2010 Comparison of Langevin and Markov channel noise models for neuronal signal generation *Phys. Rev.* E **81** 011918

[58] Goldwyn J H, Imennov N S, Famulare M and Shea-Brown E 2011 Stochastic differential equation models for ion channel noise in Hodgkin-Huxley neurons *Phys. Rev.* E **83** 041908

[59] Schmid I, Goychuk and Hänggi P 2001 Stochastic resonance as a collective property of ion channel assemblies *Europhys. Lett.* **56** 22–28

[60] Orio P and Soudry D 2012 Simple, fast and accurate implementation of the diffusion approximation algorithm for stochastic ion channels with multiple states *PLoS One* **7** e36670

[61] Dangerfield C E, Day D and Burrage K 2012 Modeling ion channel dynamics through reflected stochastic differential equations *Phys. Rev.* E **85** 1–15

[62] Huang Y D, Rüdiger S and Shuai J W 2013a Channel-based Langevin approach for the stochastic Hodgkin–Huxley neuron *Phys. Rev.* E **87** 1–9

[63] Horikawa Y 1991 Noise effects on spike propagation in the stochastic Hodgkin-Huxley models *Biol. Cybern.* **66** 19–25

[64] Gibson M A and Bruck J 2000 Efficient exact stochastic simulation of chemical systems with many species and many channels *J. Phys. Chem.* A **104** 1876–89

[65] Gillespie D T, Hellander A and Petzold L R 2013 Perspective: Stochastic algorithms for chemical kinetics *J. Chem. Phys.* **138** 170901

[66] Gillespie D T 2001 Approximate accelerated stochastic simulation of chemically reacting systems *J. Chem. Phys.* **115** 1716–33

[67] Gillespie D T 2000 The chemical Langevin equation *J. Chem. Phys.* **113** 297–306

[68] Melykuti B, Burrage K and Zygalakis K C 2010 Fast stochastic simulation of biochemical reaction systems by alternative formulations of the chemical Langevin equation *J. Chem. Phys.* **132** 164109

[69] Van Kampen N G 1992 *Stochastic Processes in Physics and Chemistry* vol 1 (Amsterdam: Elsevier)
[70] Hänggi P, Grabert H, Talkner P and Thomas H 1984 Bistable systems: Master equation versus Fokker–Planck modeling *Phys. Rev.* A **29** 371–8
[71] Bressloff P C 2010 Metastable states and quasicycles in a stochastic wilson-cowan model of neuronal population dynamics *Phys. Rev.* E **82** 051903
[72] Casado J M 2003 Synchronization of two Hodgkin–Huxley neurons due to internal noise *Phys. Lett.* A **310** 400–6
[73] Wang M, Hou Z and Xin H 2004 Double-system-size resonance for spiking activity of coupled Hodgkin–Huxley neurons *Chem. Phys. Chem.* **5** 1602–5
[74] Schmid G, Goychuk I and Hänggi P 2004 Effect of channel block on the spiking activity of excitable membranes in a stochastic Hodgkin–Huxley model *Phys. Biol.* **1** 61–66
[75] Shuai J W, Huang Y D and Rüdiger S 2010 Puff-wave transition in an inhomogeneous model for calcium signals *Phys. Rev.* E **81** 1–8 041904
[76] Mino H, Rubinstein J T and White J A 2002 Comparison of algorithms for the simulation of action potentials with stochastic sodiumchannels *Ann. Biomed. Eng.* **30** 578–87
[77] Huang Y D, Li X and Shuai J W 2015 Langevin approach with rescaled noise for stochastic channel dynamics in Hodgkin–Huxley neuron *Chin. Phys.* B in: press
[78] Huang Y D, Rüdiger S and Shuai J W 2011 Modified Langevin approach for a stochastic calcium puff model *Europhys. J.* B **83** 401–7
[79] Linaro D, Storace M and Giugliano M 2011 Accurate and fast simulation of channel noise in conductance-based model neurons by diffusion approximation *PLoS Comput. Biol.* **7** e1002247
[80] Goldwyn J H and Shea-Brown E 2011 The what and where of adding channel noise to the Hodgkin–Huxley equations *PLoS Comput. Biol.* **7** e1002247
[81] Huang Y D, Rüdiger S and Shuai J W 2013b Langevin approach for stochastic Hodgkin-Huxley dynamics with discretization of channel open fraction *Phys. Lett.* A **377** 3223–7
[82] Güler M 2013 Stochastic Hodgkin–Huxley equations with colored noise terms in the conductances *Neural Comput.* **25** 46–74
[83] Rowat P and Greenwood P E 2014 The ISI distribution of the stochastic Hodgkin–Huxley neuron Front *Comput. Neurosci* **8** 111
[84] Pezo D, Soudry D and Orio P 2014 Diffusion approximation-based simulation of stochastic ion channels: which method to use? *Front. Comput. Neurosci* **8** 1–15
[85] Laing C and Lord G J 2010 Stochastic methods in neuroscience *Stochastic Methods in Neuroscience* (Oxford: Oxford University Press)
[86] Chen Y and Ye X 2011 Projection onto a simplex arXiv:1101.6081v2
[87] Shuai J W and Jung P 2003 Langevin modeling of intracellular calcium signaling *Understanding Calcium Dynamics* (*Lecture Notes in Physics* vol 623) pp231–52
[88] Shuai J, Rose H J and Parker I 2006 The number and spatial distribution of IP_3 receptors underlying calcium puffs in Xenopus oocytes *Biophys. J.* **91** 4033–44
[89] Smith I F and Parker I 2009 Imaging the quantal substructure of single IP_3R channel activity during Ca^{2+} puffs in intact mammalian cells *Proc. Natl Acad. Sci. USA* **106** 6404–9
[90] Taufiq-Ur-Rahman A S, Falcke M and Taylor C W 2009 Clustering of $insp_3$ receptors by $InsP_3$ retunes their regulation by $InsP_3$ and Ca^{2+} *Nature* **458** 655–9
[91] Rüdiger S 2014b Excitability in a stochastic differential equation model for calcium puffs *Phys. Rev.* E **89** 062717
[92] Zhang X, Qian H and Qian M 2012 Stochastic theory of nonequilibrium steady states and its applications: Part I *Phys. Rep.* **510** 1–86
[93] Ge H, Qian M and Qian H 2012 Stochastic theory of nonequilibrium steady states: Part II. Applications in chemical biophysics *Phys. Rep.* **510** 87–118
[94] Wolynes P G, Lan Y and Papoian G A 2006 A variational approach to the stochastic aspects of cellular signal transduction *J. Chem. Phys.* **125** 124106
[95] Lan Y and Papoian G A 2007 Stochastic resonant signaling in enzyme cascades *Phys. Rev. Lett.* **98** 228301
[96] Qian H 2014 Stochastic dynamics of electrical membrane with voltage-dependent ion channel fluctuations *Europhys. Lett.* **106** 10002
[97] Liebovitch L S and Sullivan J M 1987 Fractal analysis of a voltage-dependent potassium channel from cultured mouse hippocampal neurons *Biophys. J.* **52** 979–88
[98] Korn S J and Horn R 1988 Statistical discrimination of fractal and Markov models of single-channel gating *Biophys. J.* **54** 871–7
[99] Fulinski A, Grzywna Z, Mellor I, Siwy Z and Usherwood P N R 1998 Non-Markovian character of ionic current fluctuations in membrane channels *Phys. Rev.* E **58** 919
[100] Mercik S and Weron K 1999 Statistical analysis of ionic current fluctuations in membrane channels *Phys. Rev.* E **60** 7343–8
[101] Lowen S B, Liebovitch L S and White J A 1999 Fractal ion-channel behavior generates fractal firing patterns in neuronal models *Phys. Rev.* E **59** 5970–80
[102] Liebovitch L, Scheurle D, Rusek M and Zochowski M 2001 Fractal methods to analyze ion channel kinetics *Methods* **24** 359–75
[103] Bezrukov S M and Winterhalter M 2000 Examining noise sources at the single molecular level *Phys. Rev. Lett.* **85** 202
[104] Siwy Z and Fulinski A 2002 Noise in membrane channels currents *Phys. Rev. Lett.* **89** 158101
[105] Kosinska I D and Fulinski A 2008 Brownian dynamics simulations of flicker noise in nanochannels currents *Europhys. Lett.* **81** 50006
[106] Rao C V, Wolf D M and Arkin A P 2002 Control, exploitation and tolerance of intracellular noise *Nature* **420** 231–7
[107] Shahrezaei V and Swain P S 2008 The stochastic nature of biochemical networks *Curr. Opin. Biotechnol.* **19** 369–74
[108] Wilkinson D J 2009 Stochastic modelling for quantitative description of heterogeneous biological systems *Nat. Rev. Genetics* **10** 122–33
[109] Ribrault C, Sekimoto K and Triller A 2011 From the stochasticity of molecular processes to the variability of synaptic transmission *Nat. Rev. Neurosci.* **12** 375–87
[110] Bostani N, Kessler D A, Shnerb N M, Rappel W and Levine H 2012 Noise effects in nonlinear biochemical signaling *Phys. Rev.* E **85** 011901